

Exploring water cycle dynamics by sampling multiple stable water isotope pools in a small developed landscape of Germany

N. Orlowski^{1,2}, P. Kraft¹, J. Pferdmenges and L. Breuer^{1,3}

[1]{Institute for Landscape Ecology and Resources Management (ILR), Research Centre for BioSystems, Land Use and Nutrition (IFZ), Justus-Liebig-University Giessen, Giessen, Germany}

[2]{Global Institute for Water Security, School of Environment and Sustainability, University of Saskatchewan, Saskatoon, Canada}

[3]{Centre for International Development and Environmental Research, Justus Liebig University Giessen, Germany}

Correspondence to: N. Orlowski (Natalie.Orlowski@umwelt.uni-giessen.de)

Abstract

A dual stable water isotope ($\delta^2\text{H}$ and $\delta^{18}\text{O}$) study was conducted in the developed (managed) landscape of the Schwingbach catchment (Germany). The two-year weekly to biweekly measurements of precipitation, stream, and groundwater isotopes revealed that surface and groundwater are decoupled from the annual precipitation cycle but showed bidirectional interactions between each other. Apparently, snowmelt played a fundamental role for groundwater recharge explaining the observed differences to precipitation δ -values.

A spatially distributed snapshot sampling of soil water isotopes in two soil depths at 52 sampling points across different land uses (arable land, forest, and grassland) revealed that top soil isotopic signatures were similar to the precipitation input signal. Preferential water flow paths occurred under forested soils explaining the isotopic similarities between top and subsoil isotopic signatures. Due to human-impacted agricultural land use (tilling and compression) of arable and grassland soils, water delivery to the deeper soil layers was reduced, resulting in significant different isotopic signatures. However, the land use influence

1 smoothed out with depth and soil water approached groundwater δ -values. Seasonally tracing
2 stable water isotopes through soil profiles showed that the influence of new percolating soil
3 water decreased with depth as no remarkable seasonality in soil isotopic signatures was
4 obvious at depth >0.9 m and constant values were observed through space and time.

5 Since classic isotope evaluation methods such as mean transit time calculation failed, we
6 established a hydrological model to estimate groundwater ages and flow directions within the
7 Vollnkirchener Bach subcatchment. Our model revealed that complex age dynamics exist
8 within the subcatchment and that much of the runoff must have been stored in the catchment
9 for much longer than event water.

10 Tracing stable water isotopes through the water cycle in combination with a hydrological
11 model was valuable for determining interactions between different water cycle components
12 and unravelling age dynamics within the study area. This knowledge can further improve
13 catchment specific process understanding of developed, human-impacted landscapes.

14 **1 Introduction**

15 The application of stable water isotopes as natural tracers in combination with hydrodynamic
16 methods has been proven to be a valuable tool for studying the origin, formation, and
17 interrelationship between surface water and groundwater (Blasch and Bryson, 2007; Goni,
18 2006), partitioning evaporation and transpiration (Phillips and Gregg, 2003; Rothfuss et al.,
19 2010, 2012; Wang and Yakir, 2000), and further mixing processes between various water
20 sources (Aggarwal et al., 2007; Clark and Fritz, 1997c; Kendall and Coplen, 2001; Wu et al.,
21 2012). Particularly in catchment hydrology, stable water isotopes play a major role since they
22 can be utilised for hydrograph separations (Buttle, 2006; Hoeg et al., 2000; Ladouche et al.,
23 2001; Munyaneza et al., 2012), to calculate the mean transit time (McGuire et al., 2002, 2005;
24 Rodgers et al., 2005b), to investigate water flow paths (Barthold et al., 2011; Goller et al.,
25 2005; Rodgers et al., 2005a), or to improve hydrological model simulations (Birkel et al.,
26 2010; Koivusalo et al., 1999; Liebinger et al., 2007; Rodgers et al., 2005b). However,
27 spatio-temporal sources of stream water in low angle, developed catchments are still poorly
28 understood. This is partly caused by damped stream water isotopic signatures excluding
29 traditional hydrograph separations (Klaus et al., 2015). Unlike the distinct watershed
30 components found in steeper headwater counterparts, lowland areas often exhibit a complex
31 groundwater–surface water interaction (Klaus et al., 2015). This interaction between
32 groundwater and surface water remains poorly understood in many catchments throughout the

1 world but process understanding is fundamental to effectively manage the quantity and
2 quality of water resources (Ivkovic, 2009). Sklash and Farvolden (1979) showed very early,
3 that groundwater plays an important role as a generating factor for storm and snowmelt runoff
4 processes. In many catchments, streamflow responds promptly to rainfall inputs but variations
5 in passive tracers such as water isotopes are often strongly damped (Kirchner, 2003). This
6 indicates that storm runoff in these catchments is dominated mostly by “old water” (Buttle,
7 1994; Neal and Rosier, 1990; Sklash, 1990). However, not all “old water” is the same
8 (Kirchner, 2003). This catchment behaviour was described by Kirchner (2003) as the old
9 water paradox. Thus, there is evidence of complex age dynamics within catchments and that
10 much of the runoff is stored in the catchment for much longer than event water (Rinaldo et al.,
11 2015). Still, some of the physical processes controlling the release of “old water” from
12 catchments are poorly understood, roughly modelled, and the observed data do not suggest a
13 common catchment behaviour (Botter et al., 2010).

14 Moreover, due to human-induced alterations of river systems (e.g. channelisation of
15 streambeds or draining) (O’Driscoll et al., 2010), water fluxes in developed (managed)
16 landscapes can be especially diverse. Almost all European river systems were already
17 substantially modified by humans before river ecology research developed (Klapper, 1990;
18 Allan, 2004). Through changes in land use, land cover and irrigation, agriculture has
19 substantially modified the hydrological cycle in terms of both water quality and quantity
20 (Gordon et al., 2010) as well as altered the functioning of aquatic ecosystem processes (Pierce
21 et al., 2012; Rockström et al., 2014). This complex character of developed, agricultural
22 dominated catchments is often disregarded and established research approaches often failed to
23 fully capture agro-ecosystem functioning at multiple scales (Orlowski et al., 2014). Since
24 agricultural land use (arable land, permanent crops, and grassland) is the most dominant land
25 use in Europe (UNEP, 2002), there exists a pressing need to understand biogeochemical
26 fluxes (e.g. nitrogen compounds or pesticides) coupled with water fluxes in these managed
27 landscapes (Orlowski et al., 2014) and to figure out a way to embed this landscape
28 heterogeneity or the consequence of the heterogeneity into models (McDonnell et al., 2007).

29 One way to better understand the relationship between precipitation, stream, soil, and
30 groundwater, is detailed knowledge about the isotopic composition of the different water
31 sources (surface, subsurface, and groundwater) and their variation in space and time. In
32 principal, isotopic signatures of precipitation are altered by temperature, amount (or rainout),

1 continental, altitudinal, and seasonal effects. They are mainly influenced by prevailing
2 atmospheric conditions during rainfall and snowfall causing a depletion of isotopes (Araguás-
3 Araguás et al., 2000; Blasch and Bryson, 2007; Clark and Fritz, 1997c; Gat, 1996; Rohde,
4 1998). The input signal becomes more pronounced in snow-dominated systems where
5 snowfall and snowmelt are depleted in heavy stable water isotopes relative to rainfall (Maule
6 et al., 1994; O'Driscoll et al., 2005). Stream water isotopic signatures can reflect precipitation
7 isotopic composition and moreover, depend on discharge variations affected by seasonally
8 variable contributions of different water sources such as bidirectional water exchange with the
9 groundwater body during baseflow, or high event-water contributions during stormflow
10 (Genereux and Hooper, 1998; Koeniger et al., 2009). Following the way of precipitation over
11 the unsaturated zone to the groundwater, the process of infiltration in itself is known to be a
12 non-fractionating process (Gonfiantini et al., 1998), except for mixing between different water
13 pools (e.g. moving and standing water) (Gat, 1996). However, precipitation falling on
14 vegetated areas is intercepted by plants and re-evaporated thus isotopically fractionated. The
15 remaining throughfall infiltrates slower and can be affected by evaporation resulting in an
16 enrichment of heavy isotopes, particularly in the upper soil layers (Gonfiantini et al., 1998;
17 Kendall and Caldwell, 1998). In the soil, specific isotopic profiles develop, characterized by
18 an evaporative layer near the surface especially under arid and semi-arid climate. This
19 decreases exponentially with depth (Zimmermann et al., 1968), representing a balance
20 between the upward convective flux and the downward diffusion of the evaporative signature
21 (Barnes and Allison, 1988). In humid and semi-humid areas, this exponential decrease is
22 generally interrupted by the precipitation isotopic signal. Hence, the combination of the
23 evaporation effect and the precipitation isotopic signature determine the isotope profile in the
24 soil (Song et al., 2011). Once soil water reaches the saturated zone, this isotope information is
25 finally transferred to the groundwater (Song et al., 2011). Soil water can therefore be seen as a
26 link between precipitation and groundwater, and the dynamics of isotopic composition in soil
27 water are indicative of the processes of precipitation infiltration, evaporation of soil water,
28 and recharge to groundwater (Blasch and Bryson, 2007; Song et al., 2011).

29 To compare different water sources on the catchment-scale, a local meteoric water (LMWL)
30 line is developed and evaporation water lines (EWLs) are used. They represent the linear
31 relationship between $\delta^2\text{H}$ and $\delta^{18}\text{O}$ of meteoric waters (Cooper, 1998) in contrast to the global
32 meteoric water line (GMWL), which describes the world-wide average stable isotopic
33 composition in precipitation (Craig, 1961a). Thus, the comparison of stable isotope data for

1 stream, soil, or groundwater samples relative to the global or local meteoric water lines can
2 provide general understandings on water cycle processes at specific research sites (Song et al.,
3 2011).

4 Identifying the origin of water vapour sources and moisture recycling (Gat et al., 2001; Lai
5 and Ehleringer, 2011), the deuterium-excess (d-excess), defined by Dansgaard (1964) as
6 $d = \delta^2\text{H} - 8 \times \delta^{18}\text{O}$ can be used, since the d-excess mainly depends on the mean relative
7 humidity of the air masses formed above the ocean surface (Zhang et al., 2013). In addition,
8 the d-excess reflects the prevailing conditions during evolution, interaction, or mixing of air
9 masses en route to the precipitation site (Froehlich et al., 2002).

10 To capture spatial landscape heterogeneity, but to keep data acquisition simple, stable water
11 isotope data were coupled with hydrodynamic data from a previous study by Orłowski et al.
12 (2014) in the developed Schwingbach catchment (Germany) to unravel water flow paths and
13 interactions between different water cycle components. Results obtained through this earlier
14 study imply that the Schwingbach catchment is highly responsive, indicated by fast runoff
15 responses to precipitation inputs (Orłowski et al., 2014). Moreover, groundwater reacted
16 almost as quickly as streamflow to precipitation events with raising head levels. Thus, the
17 catchment exhibited “old water” paradox like behaviour (Kirchner, 2003). We further showed
18 that streamflow was predominantly generated in the catchment headwater area and that
19 gaining and losing stream reaches occurred in parallel along the studied stream affected by the
20 underlying geology.

21 Thus, stable water isotopes in combination with hydrodynamic data of a two-year monitoring
22 period (July 2011 to July 2013) were utilised to explore spatio-temporal isotopic variations,
23 unravel linkages between the different water cycle components, investigate the
24 transformations from precipitation to soil and groundwater, and analyse the effect of small-
25 scale landscape characteristics (i.e. soil physical properties, topographic wetness index (TWI),
26 distance to stream, and vegetation cover) on soil water isotopic composition. Further, stable
27 water isotope data was utilized to estimate groundwater ages and flow directions in the
28 Vollnkirchener Bach subcatchment via an hydrological model setup based on the findings of
29 Orłowski et al. (2014).

1 2 Materials and methods

2 2.1 Study area

3 The research was carried out in the Schwingbach catchment (50°30'4.23"N, 8°33'2.82"E)
4 (Germany) (Fig. 1a). The Schwingbach and its main tributary the Vollnkirchener Bach are
5 low-mountainous creeks (Fig. 1c) with an altered physical structure of the stream system
6 (channelled stream reaches, pipes, drainage systems, fishponds). The whole Schwingbach
7 catchment encompasses an area of 9.6 km², with an altitude range from 233–415 m a.s.l. The
8 Vollnkirchener Bach tributary is about 4.7 km in length and drains a 3.7 km² subcatchment
9 area (Fig. 1c), which ranges in elevation from 235–351 m a.s.l. Almost 46% of the overall
10 Schwingbach catchment is forested, which slightly exceeds agricultural land use (35%)
11 (Fig. 1c). Grassland (10%) is mainly distributed along streams and smaller meadow orchards
12 are located around the villages.

13 The Schwingbach main catchment is underlain by argillaceous shale in the northern parts,
14 serving as aquicludes (Mazor, 2003). Graywacke zones with lydite in the central, as well as
15 limestone, quartzite, and sandstone regions in the headwater area provide aquifers with large
16 storage capacities (Choi, 1997; Mazor, 2003) (Fig. 1f). Loess covers Paleozoic bedrock at
17 north- and east bounded hillsides (Fig. 1f). Streambeds consists of sand and debris covered by
18 loam and some larger rocks (Lauer et al., 2013). Many downstream sections of both creeks
19 are framed by armor stones (Orlowski et al., 2014). Figure 1e shows that the dominant soil
20 types in the overall study area are Stagnosols (41%) and mostly forested Cambisols (38%).
21 Stagnic Luvisols with thick loess layers are under agricultural use. The same is true for
22 Regosol, Luvisols, and Anthrosols, which encompass an area of 7%. Gleysols are found
23 predominantly under grassland sites along the creeks.

24

25 [Figure 1 near here]

26

27 The climate in the study area is classified as temperate with a mean annual temperature of
28 8.2°C. An annual precipitation sum of 633 mm (for the hydrological year 1 November 2012
29 to 31 October 2013) was measured at the catchment's climate station (site 13, Fig. 1b). The
30 year 2012 to 2013 was an average hydrometeorological year. For comparison, the climate

1 station Giessen/Wettenberg (25 km N of the catchment) operated by the German
2 Meteorological Service (DWD, 2014) records a mean annual temperature of 9.6 °C and a
3 mean annual precipitation sum of 666 ± 103 mm for the period 1980 to 2010. Discharge peaks
4 from December to April (measured by the use of RBC-flumes with maximum peak flow of
5 114 L s^{-1} , Eijkelkamp Agrisearch Equipment, Giesbeek, NL) and low flows occur from July
6 until November. Substantial snowmelt peaks were observed during December 2012 and
7 February 2013. Furthermore, May 2013 was an exceptional wet month characterised by
8 discharge of $2\text{--}3 \text{ mm d}^{-1}$. A more detailed description of runoff characteristics, especially for
9 the Vollnkirchener Bach is given in a previous study by Orłowski et al. (2014).

10 **2.2 Monitoring network and water isotope sampling**

11 The monitoring network consists of an automated climate station (site 13, Fig. 1 b–c)
12 (Campbell Scientific Inc., AQ5, UK; equipped with a CR1000 data logger collecting air
13 temperature at 2 m height, wind speed and direction, relative humidity, and solar radiation),
14 three tipping buckets, 15 precipitation collectors, six stream water sampling points, and 22
15 piezometers (Fig. 1 b–c). Precipitation data were corrected according to Xia (2006).

16 Two stream water sampling points (sites 13 and 18) in the Vollnkirchener Bach are installed
17 with trapezium shaped RBC-flumes for gauging discharge (Eijkelkamp Agrisearch
18 Equipment, Giesbeek, NL) and a V-weir is located at sampling point 64. RBC-flumes and V-
19 weir are equipped with Mini-Divers® (Eigenbrodt Inc. & Co. KG, Königsmoor, DE) for
20 automatically recording water levels and deriving continuous discharge data through the
21 given stage-discharge relationships (Eijkelkamp, 2014). Discharge at the remaining stream
22 sampling points was manually measured applying the salt dilution method (WTW-cond340i,
23 WTW, Weilheim, DE), which can be precise to $\pm 5\%$ (Day, 1976; Moore, 2004). The 22
24 piezometers (Fig. 1b) situated between the conjunction of the Schwingbach with the
25 Vollnkirchener Bach and the upper RBC-flume of the Vollnkirchener Bach (site 18) are made
26 from perforated PVC tubes sealed with a bentonite clay at the upper part of the tube to
27 prevent contamination by surface water. For monitoring shallow groundwater levels, either
28 combined water level/temperature loggers (Odyssey Data Flow System, Christchurch, NZ) or
29 Mini-Diver® water level loggers (Eigenbrodt Inc. & Co. KG, Königsmoor, DE) are installed.
30 Accuracy of Mini-Diver® is ± 5 mm and for Odyssey data logger ± 1 mm. For calibration
31 purposes, groundwater levels are additionally measured manually via an electric contact
32 gauge.

1 Stable water isotope samples of rainfall, stream-, and groundwater were taken over a two-year
2 observation period (July 2011 to July 2013) approximately on weekly intervals, except for the
3 winter period. In winter 2012 to 2013, snow core samples over the entire snow depth of
4 <0.15 m were collected in tightly sealed jars at same sites as open rainfall was sampled. We
5 sampled shortly after snow was fallen because sublimation, recrystallization, partial melting,
6 rainfall on snow, and redistribution by wind can alter the primary isotopic composition of the
7 snowfall (Clark and Fritz, 1997b). Samples were melted overnight following Kendall and
8 Caldwell (1998), and analysed for their isotopic composition. Open rainfall was collected in
9 self-constructed samplers. Each collector was made from a 1 L glass bottle prepared with a
10 circular funnel of 0.10 m in diameter. Funnels were covered with a mosquito net to keep out
11 leaves, insects, or windblown debris. Bottles were placed in PVC tubes to avoid heating,
12 screwed to wooden pales, and installed 1 m above ground. To avoid sample evaporation, a
13 table tennis ball was placed into each funnel and two layers of small plastic balls were
14 inserted into the glass bottles (Windhorst et al., 2013).

15 Stream water samples were taken as grab samples at six locations – three sampling points at
16 each stream (Vollnkirchener Bach sites: 13, 18, and 94; Schwingbach sites: 11, 19, and 64)
17 (Fig. 1b–c). To account for possible spatial variation in groundwater, grab samples were
18 collected from 17 piezometers (Fig. 1b). Since spatial variations between the piezometers
19 under meadow was small, the amount of sampled piezometers was reduced to three sampling
20 points under meadow (sites 1, 6, and 21), five under the arable field (sites 25–29), and four
21 beside the Vollnkirchener Bach (sites 24, 31, 32, and 35). Additionally, a drainage pipe (site
22 15) located ~226 m downstream of site 18 was sampled. According to IAEA standard
23 procedures, all samples were filled and stored in 2 mL brown glass vials, sealed with a solid
24 lid, and wrapped up with Parafilm® (Mook, 2001).

25 **2.3 Isotopic soil sampling**

26 **2.3.1 Spatial variability**

27 In order to analyse the effect of small-scale characteristics such as distance to stream, TWI,
28 and land use on soil isotopic signatures as connecting compartment between precipitation and
29 groundwater, we sampled a snapshot of 52 points evenly distributed over a 200 m grid around
30 the Vollnkirchener Bach (Fig. 1d). Soil samples were taken at four consecutive rainless days
31 (1 to 4 November 2011) at altitudes of 235–294 m a.s.l.. Sampling sites were selected via a

1 stratified, GIS-based sampling plan (ArcGIS, Arc Map 10.2.1, Esri, California, USA),
2 including three classes of topographic wetness indices (TWIs: 4.4–6.5; 6.5–7.7; 7.7–18.4),
3 two different distances to stream (0–121 m, 121–250 m), and three land use units (arable land,
4 forest, and grassland), with each class containing the same number of sampling points.
5 Samples were collected at depths of 0.2 m and 0.5 m. Gravimetric water content was
6 measured according to DIN-ISO 11465 by drying soils for 24 h at 110 °C. Soil pH was
7 analysed following DIN-ISO 10390 on 1:1 soil-water-mixture with a handheld pH-meter
8 (WTW cond340i, WTW Inc., DE). Bulk density was determined according to DIN-ISO
9 11272, and soil texture by finger testing (Whitefield, 2004).

10 **2.3.2 Seasonal isotope soil profiling and isotope analysis**

11 In order to trace the seasonal development of stable water isotopes from rainfall to
12 groundwater, seven soil profiles were taken in the dry summer season (28 August 2011),
13 seven in the wet winter period (28 March 2013), and two profiles in the transitional season
14 spring (24 April 2013) under different vegetation cover (arable land and grassland) (Fig. 1d).
15 Soil was sampled utilising a hand-auger (Eijkelkamp Agrisearch Equipment BV, Giesbeek,
16 DE). Samples were taken from the soil surface to 2 m depth. Samples were collected in
17 greater detail near the soil surface since this area is known to have the greatest isotopic
18 variability (Barnes and Allison, 1988; Hsieh et al., 1998; Zimmermann et al., 1968).

19 Soil samples were stored in amber glass tubes, sealed with Parafilm®, and kept frozen until
20 water extraction (Orlowski et al., 2013). Soil water was extracted cryogenically with 180 min
21 extraction duration, a vacuum threshold of 0.3 Pa, and an extraction temperature of 90°C
22 following Orlowski et al. (2013). Isotopic signatures of $\delta^{18}\text{O}$ and $\delta^2\text{H}$ were analysed via off-
23 axis integrated cavity output spectroscopy (OA-ICOS) (DLT-100, Los Gatos Research Inc.,
24 Mountain View, CA, USA). Within each isotope analysis three calibrated stable water isotope
25 standards of different water isotope ratios were included (LGR working standard number 1, 3,
26 and 5; Los Gatos Research Inc., CA, US). After every fifth sample the LGR working
27 standards are measured. For each sample, six sequential 900 μL aliquot of a water sample are
28 injected into the analyser. Then, the first three measurements are discarded. The remaining are
29 averaged and corrected for per mil scale linearity following the IAEA laser spreadsheet
30 template (Newman et al., 2009). Following this IAEA standard procedure allows for drift and
31 memory corrections. Isotopic ratios are reported in per mil (‰) relative to Vienna Standard
32 Mean Ocean Water (VSMOW) (Craig, 1961b). Accuracy of analyses was 0.6‰ for $\delta^2\text{H}$ and

1 0.2‰ for $\delta^{18}\text{O}$ (LGR, 2013). Leaf water extracts typically contain a high fraction of organic
2 contaminations (West et al., 2010), which might lead to spectral interferences when using
3 isotope ratio infrared absorption spectroscopy (Leen et al., 2012), causing erroneous isotope
4 values (Schultz et al., 2011). Therefore, isotopic data of plant water extracts are usually
5 checked for spectral interferences using the Spectral Contamination Identifier (LWIA-SCI)
6 post-processing software (Los Gatos Research Inc.). However, for soil water extracts no
7 evidence for such interferences have been observed so far (Schultz et al., 2011; Zhao et al.,
8 2011). Thus, there exists no need to check or correct such data.

9 **2.4 Mean transit time estimation**

10 To understand the connectivity between the different water cycle components in the
11 Schwingbach catchment, the mean transit times (MTT) for the Vollnkirchner Bach (sites 13,
12 18, and 94) and the Schwingbach (sites 11, 19, and 64) were calculated using FlowPC
13 (Małoszewski and Zuber, 1996). Different models (dispersion model with different dispersion
14 parameters $D_p = 0.05, 0.4, \text{ and } 0.8$, exponential model, exponential-piston-flow model, linear
15 model, and linear-piston-flow model) were compared for their results (sigma as goodness of
16 fit and model efficiencies (ME)). A model efficiency $ME = 1$ indicates an ideal fit of the
17 model to the concentrations observed, while $ME = 0$ indicates that the model fits the data no
18 better than a horizontal line through the mean concentration observed (Maloszewski and
19 Zuber, 2002). The same is true for sigma.

20 For calculations with FlowPC, weekly averages of precipitation and stream water isotopic
21 signatures were calculated. We also bias-corrected the precipitation input data with two
22 different approaches: the mean precipitation value was subtracted from every single
23 precipitation value and then divided by the standard deviation of precipitation isotopic
24 signatures. Afterwards, this value was subtracted from the weekly precipitation values (bias1).
25 For the second approach, the difference of the mean stream water isotopic value and the mean
26 precipitation value was calculated and also subtracted from the weekly precipitation values
27 (bias2).

28 **2.5 Hydrological model setup**

29 To estimate the age dynamics of the groundwater body in the Vollnkirchner Bach
30 subcatchment, a hydrological model was established on the basis of the conceptual model

1 presented by Orłowski et al. (2014). For this purpose the *Catchment Modelling Framework*
2 (CMF) by Kraft et al. (2011) was used. CMF is a modular framework for hydrological
3 modelling based on the concept of finite volume method by Qu and Duffy (2007). CMF is
4 applicable for simulating one- to three-dimensional water fluxes but also advective transport
5 of stable water isotopes (^{18}O and ^2H). Thus, it is especially suitable for our tracer study and
6 can be used to study the origin (Windhorst et al., 2014) and age of water.

7 The generated model is a highly simplified representation of the Vollnkirchener Bach
8 subcatchment's groundwater body. The subcatchment is divided into 353 polygonal shaped
9 cells ranging from 101.7–38940.1 m², manually adjusted on the basis of land use, soil types,
10 and contour lines following Qu and Duffy (2007) and Windhorst et al. (2014). Each cell
11 contains two layers, one comprises a water storage. The upper layer, representing the
12 groundwater body, is generated based on soil depth measurements and reaches down to 20 m
13 below the surface. Due to the fact that groundwater depth was not measured, the layer-
14 thickness is a rough estimation. The second layer (20–40 m below the surface) represents the
15 bedrock. The main fresh water input is the groundwater recharge, which is a constant value
16 over time for each cell. It is calculated as the difference between rainfall, evapotranspiration,
17 and the change in stored water. Precipitation and evapotranspiration values are calculated
18 using a fully distributed 3D model established through CMF with a one year simulation
19 period of the same subcatchment. The change in stored water is set to zero since a steady state
20 is simulated (see below) and therefore the water content in the system is stable.

21 Besides the groundwater recharge, a combined sewer overflow (site 38) is considered as an
22 additional water input based on findings of Orłowski et al. (2014). Moreover, there are two
23 water outlets in the two lowest cells for efficient draining. Both cells are located in the very
24 north of the subcatchment. The compartments within the system are linked by a series of
25 flow-accounting equations: Richards equation for percolation, Darcy equation for lateral
26 subsurface flow, Neumann boundary condition for input of fresh water (groundwater
27 recharge, pipe source), and constant Dirichlet boundary conditions representing the system
28 outlets.

29 For estimating the groundwater age, a virtual tracer is used. It is modelled as a radioactive
30 decay tracer with a fixed concentration at the input to the system. From the modelled
31 concentration of the tracer in each cell, the mean age of the water for this cell is derived.

1 Model assumptions: The saturated hydraulic conductivity of the groundwater body is set to
2 0.1007 m d^{-1} , as measured in the study area. For the bedrock compartment there is no data
3 available. However, expecting a high rate of joints, preliminary testing revealed that a
4 saturated hydraulic conductivity of 0.25 m d^{-1} seemed to be a realistic estimation (based on
5 field measurements).

6 **2.6 Statistical analyses**

7 For statistical analyses, we used IBM SPSS Statistics (Version 22, SPSS Inc., Chicago, IL,
8 US) and R (version Rx64 3.2.2). The R package igraph was utilized for plotting (Csardi and
9 Nepusz, 2006). Studying temporal and spatial variations in meteoric and groundwater, isotope
10 data were tested for normal distribution. Subsequently, t-tests or Multivariate Analyses of
11 Variances (MANOVAs) were applied and Tukey-HSD tests were run to determine which
12 groups were significantly different ($p \leq 0.05$). Event mean values of isotopes in precipitation,
13 stream, and groundwater were calculated when no spatial variation was observed.

14 We used a topology inference network map (Kolaczyk, 2014) in combination with a principal
15 component analysis (Jolliffe, 2002) to show $\delta^{18}\text{O}$ isotope relationships between surface and
16 groundwater sampling points. To explore the sensitivity of missing data, we used both the
17 complete isotope time series and randomly selected 80% of the whole data sets. Overall, the
18 cluster relationships of the surface and groundwater sampling points are largely similar for
19 both whole and subsets of isotope data sets, despite some differences of the exact cluster
20 centroid locations. We therefore decided to use randomly selected 80% of the isotope time
21 series to illustrate our results. In the network map, each node of the network represents an
22 isotope sampling point. The locations of the nodes are based on the first two components
23 (PC1 and PC2). The correlations between isotope time series are represented by the edges
24 connecting nodes. The thickness of edges characterizes the strength of the correlations. The p-
25 values of correlations are approximated by using the F-distributions and mid-ranks are used
26 for the ties (Hollander et al., 2013). Only statistically significant connections ($p < 0.05$) are
27 shown in the network diagram. Basic background information related to graph theory can be
28 found in Wallis (2007).

29 For comparisons, precipitation isotope data from the closest GNIP (Global Network of
30 Isotopes in Precipitation) station Koblenz (DE; 73.8 km SW of the study area, 97 m a.s.l) was
31 used (IAEA, 2014; Stumpp et al., 2014). For monthly comparisons with Schwingbach d-

1 excess values, we used a data set from the GNIP station Koblenz that includes 24 values
2 starting from July 2011 to July 2013.

3 **3 Results**

4 Descriptive statistics of isotopic composition in precipitation, stream-, and groundwater are
5 shown along with d-excess values in Table 1 and are described in detail in the following:

6

7

[Table 1 near here]

8

9 **3.1 Variations of precipitation isotopes and d-excess**

10 The $\delta^2\text{H}$ values of all precipitation isotope samples ($N = 592$) taken throughout the
11 observation period (July 2011 to July 2013) ranged from -167.6 to -8.3‰ . To examine the
12 spatial isotopic variation, rainfall was collected at 15 open field site locations throughout the
13 Schwingbach main catchment (Fig. 1b–c) for a 7-month period. However, no spatial variation
14 could be observed in the Schwingbach catchment. Thus, rainfall was collected at the
15 catchment outlet (site 13) from 23 October 2014 onward and event mean δ -values were
16 calculated for the previous isotope data.

17 Analysing effects that influence the isotopic composition of precipitation, neither an amount
18 effect nor an altitude effect was found – not surprisingly, as the greatest altitudinal difference
19 between sampling points was only 101 m. Nevertheless, a slight temperature effect ($R^2 = 0.5$
20 for $\delta^2\text{H}$ and $R^2 = 0.6$ for $\delta^{18}\text{O}$, respectively) was observed showing enriched isotopic
21 signatures at higher temperatures.

22 Strong temporal variations in precipitation isotopic signatures, as well as pronounced seasonal
23 isotopic effects were measured with greatest isotopic differences occurring between summer
24 and winter. Samples taken in the fall and spring were isotopically similar, however, differed
25 from winter isotopic signature, which were somewhat lighter (Fig. 2). Furthermore, in the
26 winter of 2012–13 snow could be sampled, which decreased the mean winter isotopic values
27 for this period in comparison to the previous winter period (2011–12). No statistically
28 significant ($p > 0.05$) inter-annual variation was detected between the summer periods of 2011
29 and 2012 (Fig. 2), which could have reflected varying local climate conditions (Koeniger et
30 al., 2009).

1

2

[Figure 2 near here]

3

4 Examining the influence of moisture recycling on the isotopic compositions of precipitation,
5 the deuterium-excess (d-excess) was calculated for each individual rain event at the
6 Schwingbach catchment. For the two-year observation period, d-excess values (N = 108)
7 ranged from -7.8‰ to $+19.4\text{‰}$ and averaged $+7.1\text{‰}$ (Fig. 2). In general, 37% of all events
8 were sampled in summer periods (21 June to 21/22 September) and showed lower d-excess
9 values in comparison to the 19% winter precipitation events (21/22 December to 19/20
10 March) (Fig. 2). D-excess greater than $+10\text{‰}$ was determined for 22% of all events. As a
11 reference the d-excess of the GMWL $d = 10$ is depicted in Figure 2 (solid line). Lowest values
12 corresponded to summer precipitation events with evaporation of the raindrops below the
13 cloud base at mean daily air temperatures between $12\text{--}18^\circ\text{C}$. Most of the higher values
14 ($>+10\text{‰}$) appeared in cold seasons (fall/winter) and winter snow samples of the Schwingbach
15 catchment with very depleted δ -values showed highest d-excess values (Fig. 2).

16 In comparison with the GNIP station Koblenz (years 2011–2013), the mean annual d-excess
17 at the Schwingbach catchment was on average 3.9‰ higher (7.1‰ for 2011–12 and 2012–13,
18 respectively), showing a greater impact of oceanic moisture sources than the further south-
19 west located station Koblenz. The unweighted mean annual d-excess at the GNIP station
20 Koblenz was 2.9‰ for July 2011 to June 2012 and 3.6‰ for July 2012 to June 2013, whereas
21 the long-term mean was 4.4‰ (1978–2009) (Stumpp et al., 2014). Nevertheless, highest d-
22 excesses at the GNIP station matched highest values in the Schwingbach catchment, both
23 occurring in the cold seasons (October to December 2011 and November to December 2012).
24 Since no amount effect on the $\delta^2\text{H}$ and $\delta^{18}\text{O}$ values was observed in the Schwingbach, also no
25 linear regression of event d-excess with precipitation amount was detected.

26 The linear relationship of $\delta^2\text{H}$ and $\delta^{18}\text{O}$ content in local precipitation, results in a local
27 meteoric water line (LMWL) (Fig. 3), which can be utilised to link the relative contribution of
28 seasonal precipitation to ground and surface water sources (Wassenaar et al., 2011). The
29 global meteoric water line (GMWL) established by Craig (1961a), and more recently refined
30 by Rozanski et al. (1993) is $\delta^2\text{H} = 8.13 \times \delta^{18}\text{O} + 10.8 \text{‰}$, provides a valuable benchmark
31 against which regional or local waters can be compared (Song et al., 2011). The slope of the
32 LMWL of the Schwingbach catchment is well in agreement with the one from the closest

1 GNIP station in Koblenz ($\delta^2\text{H} = 7.66 \times \delta^{18}\text{O} + 2.0 \text{‰}$; $R^2 = 0.97$; 1978–2009 (Stumpp et al.,
2 2014)), but is slightly lower in comparison to the revised GMWL, showing stronger local
3 evaporation conditions. Since evaporation causes a differential increase in $\delta^2\text{H}$ and $\delta^{18}\text{O}$
4 values of the remaining water, the slope for the linear relationship between $\delta^2\text{H}$ and $\delta^{18}\text{O}$ is
5 lower in comparison to the GMWL (Rozanski et al., 2001; Wu et al., 2012). The lower
6 intercept (d-excess), dependent on the humidity and temperature conditions in the evaporation
7 region (Mook, 2001), nevertheless shows that moisture recycling did obviously not play a
8 major role in the study area.

9

10 [Figure 3 near here]

11

12 Considering isotope samples of the different water cycle components in comparison with the
13 LMWL revealed that mean isotope values of snow samples were for $\delta^2\text{H}$ approximately 84‰
14 lighter than mean precipitation isotopic signatures (Fig. 3). Stream water isotope samples of
15 both creeks (Schwingbach and Vollnkirchener Bach) fell on the LMWL, showing slight
16 evaporative enrichment for few samples (Fig. 3). Moreover, isotopic values for stream water
17 were almost identical to those found in groundwater (Table 1, Fig. 3).

18 **3.2 Isotopes of soil water**

19 **3.2.1 Spatial variability**

20 Determining the impact of landscape characteristics on soil water isotopic signatures, we
21 found no relationship between the parameters distance to stream, TWI, soil water content, soil
22 texture, pH, and bulk density with the soil isotopic signatures in two depths (0.2 and 0.5 m),
23 except for land use. This was potentially attributed to the small variation in soil textures
24 (mainly clayey silts and loamy sandy silts), bulk densities, and pH values for both soil depths
25 (Table 2). Water contents showed the greatest standard deviation within the two soil depths
26 (Table 2), however, exhibited no effect on soil water isotopes. Moreover, no tendency of
27 higher TWI values with decreasing distance to stream was obvious. Distances to the stream
28 are linked to water flow path lengths and were therefore supposed to be a controlling factor.
29 However, no impact of different distances to the stream on soil water isotopic signatures
30 could be observed.

1

2

[Table 2 near here]

3

4 The mean δ -values in the top 0.2 m of the soil profile is higher than further below, reflecting a
5 stronger impact of precipitation in the topsoil (Table 2, Fig. 4). The δ -values of top soil and
6 precipitation did not vary significantly statistically ($p>0.05$), which is not the case for
7 precipitation and subsoil (Fig. 4). Subsoil isotopic values were statistically equal to stream
8 and groundwater isotopic values (Fig. 4).

9

10

[Figure 4 near here]

11

12 Generally, all soil water isotopic values fell on the local meteoric water line, indicating no
13 evaporative enrichment of soil water (Fig. 5). Comparing soil isotopic signatures between
14 different land covers showed generally higher and statistically significantly different δ -values
15 ($p \leq 0.05$) at 0.2 m soil depth under arable land as compared to forests and grasslands.
16 However, all top soil isotopic values reflected precipitation isotopic signals (Fig. 5, top). For
17 the lower 0.5 m of the soil column, isotopic signatures under all land use units showed
18 statistically similar values; nevertheless, differing significantly from precipitation ($p \leq 0.05$)
19 (Fig. 5, bottom).

20

21

[Figure 5 near here]

22

23 Comparing soil water $\delta^2\text{H}$ values between top and subsoil under different land use units
24 showed significant differences ($p \leq 0.05$) under arable and grassland but not under forested
25 sites (Fig. 5, capital letters).

26 **3.2.2 Seasonal isotope soil profiling**

27 Isotope compositions of soil water varied seasonally: More depleted soil water was found in
28 the winter and spring (Fig. 6); contrary, soil water was enriched in summer due to evaporation
29 during warmer and drier periods (Darling, 2004). For summer soil profiles in the

1 Vollnkirchener subcatchment, no evidence for evaporation was obvious below 0.4 m soil
2 depth. However, snowmelt isotopic signatures could be traced down to a soil depth of 0.9 m
3 during spring rather than winter, pointing to a depth-translocation of meltwater in the soil,
4 more remarkable for the deeper profile under arable land (Fig. 6, upper left panel).
5 Furthermore, shallow soil water (<0.4 m) showed larger standard deviations with values
6 closer to mean seasonal precipitation inputs (Fig. 6, upper panels). Winter profiles exhibited
7 somewhat greater standard deviations in comparison to summer isotopic soil profiles. The
8 observed seasonal amplitude smoothed out with depth as soil water isotope signals
9 approached groundwater average. Generally, deeper soil water isotope values were relatively
10 constant through time and space.

11

12

[Figure 6 near here]

13

14 **3.3 Isotopes of stream water**

15 Analysing spatial differences in isotopic compositions between Schwingbach (sites 11, 19,
16 and 64) and Vollnkirchener Bach (sites 13, 18, and 94) stream water resulted in no
17 statistically significant differences for all sampling points (Fig. 7). In general, $\delta^{18}\text{O}$ values
18 varied for the Vollnkirchener Bach by $-8.4\pm 0.4\text{‰}$ and for the Schwingbach by $-8.4\pm 0.6\text{‰}$
19 over the two-year observation period (Table 1).

20

21

[Figure 7 near here]

22

23 Stream water isotopic signatures in the Schwingbach catchment were by approximately
24 -15‰ in $\delta^2\text{H}$ more depleted than precipitation signatures (Table 1). However, surface water
25 isotopic compositions were similar to groundwaters (Table 1).

26 Examining temporal isotopic variations, damped seasonality (less variation) of the isotope
27 concentration in stream water in comparison to precipitation was measured with main
28 seasonal differences occurring between summer and winter periods (Fig. 7). Most outlying
29 depleted stream water isotopic signatures (e.g. in March 2012 and 2013) could be explained

1 by snowmelt (Fig. 7). However, the outlier at the Schwingbach stream water sampling site 64
2 (-66.7‰ for $\delta^2\text{H}$) is by 8.5‰ more depleted than the two-year average of Schwingbach
3 stream water (Table 1). Rainfall falling on 24 September 2012 was -31.9‰ for $\delta^2\text{H}$. This
4 period in September was generally characterized by low flow and little rainfall (antecedent
5 precipitation index: AP8 was 8mm). Thus, little contribution of new water was observed and
6 stream water isotopic signatures were groundwater-dominated. For site 13, the outlier in May
7 2012 (-44.2‰ for $\delta^2\text{H}$) was by 13.8‰ more enriched than the average stream water isotopic
8 composition of the Vollnkirchener Bach over the two-year observation period (Table 1). A
9 runoff peak at site 13 of 0.152 mm d^{-1} and a 2.9 mm rainfall event were recorded on 23 May
10 2012. Moreover, AP8 was 23.2 mm. Thus, this outlier could be explained by precipitation
11 contributing to stream flow causing more enriched isotopic values in stream water, which
12 approached average precipitation δ -values (-43.9 ± 23.4).

13 Calculated MTT for the Schwingbach ranged between 52 and 67 weeks and for the
14 Vollnkirchener Bach between 47 and 66 weeks, whereby linear and exponential models
15 provided the best fits for all sampling points. However, the calculated output data did not fit
16 the observed values in terms of the quality criterion sigma and model efficiency (Timbe et al.,
17 2014). Model efficiencies for the Schwingbach sampling points were -0.1 – 0.0 and for the
18 Vollnkirchener Bach 0.0 – 0.4 . Sigma values for all sampling points were 0.1 for the best fit
19 models, respectively. Even a bias correction of the input data (precipitation) did not improve
20 the model outputs (sigma = 0.1). Therefore, we conclude that the application of MTT
21 estimation methods based on stable water isotopes failed in the Schwingbach catchment and
22 developed a new data-driven groundwater model to simulate observed stable water isotope
23 data.

24 **3.4 Isotopes of groundwater**

25 Since groundwater head levels responded almost as quickly as streamflow to rainfall events,
26 rainfall isotopic signatures were assumed to be rapidly transferred to the groundwater. This
27 was likewise underlined by the fact that Orłowski et al. (2014) observed bidirectional water
28 interactions between the groundwater body and the stream. Studying groundwater isotopic
29 signatures at the downstream section of the Vollnkirchener Bach, almost constant isotopic
30 values (Fig. 8, Table 1) throughout the study period were observed ($\delta^2\text{H}$: $-57.6\pm 1.6\text{‰}$ for
31 piezometers under meadow). Most depleted groundwater isotopic values ($< -80\text{‰}$ for $\delta^2\text{H}$)
32 were measured for piezometer 32 during snowmelt events in March and April 2013 as well as

1 for piezometer 27 from December 2012 to February 2013. As shown by Orłowski et al.
2 (2014) piezometer 32 is highly responsive to rainfall-runoff events and groundwater head
3 elevations showed significant correlations with mean daily discharge at this site. Further,
4 effluent conditions and lowest K_{sat} values ($7\text{--}14 \text{ mm h}^{-1}$) were measured in this stream section
5 (piezometers 32–35) (Orłowski et al., 2014).

6 In the Schwingbach catchment, groundwater under meadow differed from mean precipitation
7 values by about -14‰ for $\delta^2\text{H}$ showing no evidence of a rapid transfer of rainfall isotopic
8 signatures to the groundwater.

9

10 [Figure 8 near here]

11

12 Due to different water flow paths of groundwater along the studied stream, distinguished
13 groundwater isotopic signatures were assumed to be found. In fact, we could identify spatial
14 statistical differences between grassland and arable land groundwater isotopic signatures (Fig.
15 9). Groundwater isotopic signatures under arable land (sites: 25–29, Fig. 1b) showed more
16 enriched values (Fig. 8) and showed significant correlations ($p < 0.05$) among each other (Fig.
17 9). Arable land groundwater plotted furthest away from surface water sampling points in our
18 network map, showing no significant correlations to either the Schwingbach or the
19 Vollnkirchener Bach. This hydrological disconnectivity was already observed in the study of
20 Orłowski et al. (2014). In general, $\delta^{18}\text{O}$ time series of piezometers along the stream and under
21 the meadow showed close relations to surface water sampling points (Fig. 9). We further
22 found high correlations ($R^2 > 0.6$) of $\delta^{18}\text{O}$ time series of piezometers located under the meadow
23 (sites: 3, 6, and 21) among each other. Additionally, $\delta^{18}\text{O}$ values of piezometer 3 correlated
24 significantly ($p < 0.05$) with surface water sampling points 18 and 94 ($R^2 = 0.6$ and 0.8 ,
25 respectively) and piezometer 32 with sampling points 13 and 64 ($R^2 = 0.8$ and 0.6 ,
26 respectively).

27

28 [Figure 9 near here]

29

1 We further observed close relations ($p < 0.05$) among $\delta^{18}\text{O}$ values of Vollnkirchener Bach
2 sampling sites 13, 18, and 94 as well as of Schwingbach sites 11, 19, and 64 along with
3 correlations between each other.

4 **3.4.1 Modelled groundwater age**

5 Since MTT calculations failed, we modelled the groundwater age in the Vollnkirchener Bach
6 subcatchment using CMF, involving observed hydrometric as well as stable water isotope
7 data (Fig. 10).

8

9 [Figure 10 near here]

10

11 The maximum age of water is highly variable throughout the subcatchment, which results in a
12 very heterogeneous spatial age distribution. The groundwater in most of the outer cells is very
13 young (0–10 years), whereas the inner cells, which incorporate the Vollnkirchner Bach,
14 contain older water (>30 years). The oldest water (≥ 55 years) can be found in the Northern
15 part of the catchment (Fig. 10, detail view), where the Vollnkirchner Bach drains into the
16 Schwingbach. The main outlets of the subcatchment (dark red coloured cell and green cell)
17 even reach an age of 100 and 55 years, respectively. This can be explained by the fact that
18 these are the lowest cells within the subcatchment. Thus, water flows from the higher to the
19 lower cells and water from the whole subcatchment accumulates at these cells. The overall
20 flow path to these cells is the longest and as a consequence the groundwater age of these cells
21 is the highest.

22 In general, six cells contain groundwater that is older than 50 years (1.7% of cells), and two
23 cells reveal ages >70 years (0.6%). In contrast, 47 cells (13.3%) contain water with an age of
24 less than one year and 52.4% with an age <15 years. Thus, most of the cells contain young to
25 moderately old water (<15 years), while few cells comprise old water (>50 years). The
26 average groundwater age in the Vollnkirchener Bach subcatchment is 16 years. Relating the
27 groundwater age to the distance to the stream, we found a linear correlation ($R^2 = 0.3$) with a
28 distinct trend: The water tends to be younger with greater distance to the stream.

1 The modelled main flow direction is towards the Vollnkirchener Bach (Fig. 10). The amount
2 of flowing water depicted by the length of the arrows is generally higher near the stream,
3 whereas in most of the outer cells the amount of water is very low (Fig. 10).

4 **4 Discussion**

5 **4.1 Variations of precipitation isotopes and d-excess**

6 Analysing effects that influence the precipitation isotopic composition, no spatial variation in
7 precipitation isotopes was observed throughout the Schwingbach catchment. Mook et al.
8 (1974) also observed for north-western Europe that precipitation collected over periods of 8
9 and 24 h from three different locations within 6 km² at the same altitude were consistent
10 within 0.3‰ for δ¹⁸O. Further, no amount or altitude effect for isotopes in precipitation was
11 found. However, the observed linear relationship ($\delta^{18}\text{O} = 0.44T - 12.05\text{‰}$) between air
12 temperature and precipitation δ¹⁸O values compares reasonably well with a correlation
13 reported by Yurtsever (1975) based on north Atlantic and European stations from the GNIP
14 network $\delta^{18}\text{O} = (0.521 \pm 0.014)T - (14.96 \pm 0.21)\text{‰}$. Rozanski et al. (1982) calculated
15 $\delta^2\text{H} = (2.4 \pm 0.3)T - (80.5 \pm 4.2)\text{‰}$ ($R^2 = 0.89$) at the GNIP station Stuttgart, which is located
16 196 km South of the Schwingbach study area. This relationship is similar to the correlation
17 found for the Schwingbach catchment. Stumpp et al. (2014) analysed long-term precipitation
18 data from meteorological stations across Germany and found that 23 out of 24 tested stations
19 showed a positive long-term temperature trend over time, whereas the precipitation amount
20 was not a key factor for explaining isotope distributions or average values in German
21 precipitation. The temperature–isotope relationship was likewise strongly influenced by
22 seasonality (Stumpp et al., 2014). For the Schwingbach catchment, 53% of the events were
23 sampled at mean daily temperatures >10°C, resulting in a slight overrepresentation of values
24 measured at warmer temperatures. Nevertheless, the observed correspondence between the
25 degree of isotope depletion and the temperature reflects the influence of the temperature effect
26 in the Schwingbach catchment, which mainly appears in continental, middle–high latitudes
27 (Jouzel et al., 1997; Wu et al., 2012). Furthermore, the correlation between δ²H in monthly
28 precipitations and local surface air temperature becomes increasingly stronger towards the
29 centre of the continent (Rozanski et al., 1982).

30 Thus, the observed inter-seasonal differences in precipitation δ-values in the Schwingbach
31 catchment could mainly be attributed to seasonal differences in air temperature and water

1 vapour and their effect on evaporation (Schürch et al., 2003) and the presence of snow in the
2 winter of 2012–13 (Fig. 2). This observation is well in agreement with Gat et al. (2001) who
3 stated that for temperate climates the $\delta^{18}\text{O}$ values generally do not vary by more than 1‰
4 inter-annually, and a large part of the spread is caused by variations in the average annual
5 temperature. Moreover, the interior of the continent is obviously far more stable with regard
6 to isotopic inputs than areas under greater influence of Atlantic weather patterns. Perhaps in
7 view of this stability, only few isotope data are available for this region, apart from the
8 general GNIP-maps (Bowen and Wilkinson, 2002; Darling, 2004; IAEA, 2014) and recent
9 work (Stumpp et al., 2014), for which this work contributes valuable information.

10 Considering d-excess values, it is well-known that precipitation events originating from
11 oceanic moisture show d-excess values close to +10‰ (Craig, 1961a; Dansgaard, 1964; Wu
12 et al., 2012) and one of the main sources for precipitation in Germany is moisture from the
13 Atlantic Ocean (Stumpp et al., 2014). Lowest values corresponded to summer precipitation
14 events with evaporation of the raindrops below the cloud base at mean daily air temperatures
15 between 12–18°C. Same observations were made by Rozanski et al. (1982) for European
16 GNIP stations. Accordingly, even more negative summer d-excess values were measured at
17 air temperatures around 26–27°C for a study site in Greece (Argiriou and Lykoudis, 2006).
18 Most of the higher values measured in the Schwingbach catchment (>+10‰) appeared in cold
19 seasons (fall/winter) (Fig. 2), similar to d-excess values observed by Wu et al. (2012) for a
20 continental, semi-arid study area in Inner Mongolia (China). Winter snow samples of the
21 Schwingbach catchment with very depleted δ -values showed highest d-excess values, which
22 was again well in agreement with results of Rozanski et al. (1982) for European GNIP
23 stations. Continental precipitation events originating from oceanic moisture can approach d-
24 excess values of +10‰ (Wu et al., 2012) (Fig. 2, solid line). Air mass trajectories at
25 intercontinental, southern and eastern regions are suggested to be more stable with less
26 variable moisture sources in these regions compared to sites near the coast (Stumpp et al.,
27 2014). Therefore, rainout histories on the continent itself are more stable (Stumpp et al.,
28 2014). The observed differences in d-excess values between the Schwingbach catchment and
29 the GNIP station Koblenz can be attributed to differences in elevation range and the different
30 regional climatic settings at both sites (Koblenz is located in the relatively warmer Rhine river
31 valley). Further, no amount effect on d-excess could be determined for the Schwingbach
32 catchment, which generally occurs most likely in the tropics (Bony et al., 2008) or for intense
33 convective rain events (Gat et al., 2001) at monsoon-dominated sites (Risi et al., 2008).

1 **4.2 Isotopes of soil water**

2 **4.2.1 Spatial variability**

3 Determining potential relationships between small-scale characteristics such as distance to
4 stream, TWI, and land use on soil isotopic signatures, no tendency of higher TWI values with
5 decreasing distance to stream was obvious. Garvelmann et al. (2012) investigated two
6 hillslopes in a humid 0.9 km² catchment in the southern Black Forest (Germany) and found
7 that soil profiles upslope or with a weak affinity for saturation (low TWIs) preserved the
8 precipitation isotopic signal. In our study, the δ -values of top soil and precipitation did not
9 vary significantly statistically (Fig. 4), which is not the case for precipitation and subsoil. A
10 mixing and homogenization of new and old soil water with depth could not clearly be seen in
11 0.5 m soil depth, which would have resulted in a lower standard deviation (Song et al., 2011),
12 but standard deviations of isotopic signatures in top and subsoil were similar (Table 2).
13 Subsoil isotopic values were statistically equal to stream and groundwater isotopic values
14 (Fig. 4) implying that the catchment was under baseflow conditions during the sampling
15 campaign and that capillary rise of groundwater occurred. Nevertheless, the rainfall isotopic
16 signal was not directly transferred through the soil to the groundwater body, even so prompt
17 groundwater head level raises as a result of rainfall-runoff events occurred. This supports the
18 assumption of double paradox-like catchment behaviour.

19 Garvelmann et al. (2012) obtained high resolution $\delta^2\text{H}$ vertical depth profiles of pore water at
20 various points along two fall lines of a pasture hillslope in the southern Black Forest
21 (Germany) by applying the H₂O(liquid)–H₂O(vapor) equilibration laser spectroscopy method.
22 The authors showed that groundwater was flowing through the soil in the riparian zone
23 (downslope profiles) and dominated streamflow during baseflow conditions. Their
24 comparison indicated that the percentage of pore water soil samples with a very similar
25 stream water $\delta^2\text{H}$ signature is increasing towards the stream channel (Garvelmann et al.,
26 2012). In contrast, we found no relationship between the distance to stream and soil isotopic
27 values in the Vollnkirchener Bach subcatchment over various heights above sea level (235–
28 294 m a.s.l.).

29 Comparing soil water $\delta^2\text{H}$ values between top and subsoil under different land use units
30 showed significant differences ($p \leq 0.05$) under arable and grassland but not under forested
31 sites (Fig. 5). This could be explained through the occurrence of vertical preferential flow

1 paths and interconnected macropore flow such as continuous root channels or earthworm
2 burrows (Buttle and McDonald, 2002) characteristic for forested soils (Alaoui et al., 2011).
3 Alaoui et al. (2011) showed that macropore flow with high interaction with the surrounding
4 soil matrix occurred in forest soils, while macropore flow with low to mixed interaction with
5 the surrounding soil matrix dominates in grassland soils. The authors attributed the low
6 efficiency of grassland soil macropores in transporting all water vertically downward to the
7 fine and dense few topsoil layers caused by the land use that limit water flux into the
8 underlying macropores. In general, the upper part of most agricultural human-impacted soils
9 is restructured annually due to seasonal tilling, whereas the structure of forest soils, may
10 remain unchanged for years and be uninterrupted throughout the entire soil profile (in
11 particular macropores and biopores) (Alaoui et al., 2011). Considering the bulk density in the
12 Schwingbach catchment increasing values from forest (1.10 g cm^{-3}) over grassland
13 (1.25 g cm^{-3}) to arable land soils (1.41 g cm^{-3}) were measured in the top soil. As reported in a
14 study by Price et al. (2010) for North Carolina (USA), soils underlying forest trees generally
15 feature low bulk density in a comparison with soils impacted by human land use. The reduced
16 hydrological connectivity between top and subsoil under arable and grassland observed in the
17 Vollnkirchener Bach subcatchment therefore led to different isotopic signatures (Fig. 5).

18 Although, vegetation cover has been proven to have an impact on soil water isotopes
19 (Brodersen et al., 2000; Gat, 1996; Li et al., 2007), only few data are available for Central
20 Europe (Darling, 2004). Burger and Seiler (1992) found that soil water isotopic enrichment
21 under spruce forest in Upper Bavaria was double that beneath neighbouring arable land.
22 However, soil water isotopic signatures were not comparable to groundwater isotope values
23 (Burger and Seiler, 1992). Brodersen et al. (2000) reported the effect of vegetation structure
24 on $\delta^{18}\text{O}$ values of rainwater and soil water in the unsaturated zone in southern Germany. In
25 their study, throughfall isotopic signatures of different tree species (spruce and beech) seemed
26 to have a negligible effect on soil water isotopes, since soil water in the upper layers followed
27 the seasonal trend in the precipitation input and had a very constant signature in greater depth.
28 In contrast, Gehrels et al. (1998) detected slightly heavier isotopic signatures under forested
29 sites at a field site in the Netherlands in comparison to non-forested sites (grassland and
30 heathland), both showing isotopic signatures comparable to precipitation signals. For the
31 Schwingbach catchment, we conclude that the observed land use effect in the upper soil
32 column is mainly attributed to different preservation and transmission of the precipitation
33 input signal. It is most likely not attributed to distinguished throughfall isotopic signatures

1 since top soil water isotopic signals followed the precipitation input signal under all land use
2 units. The precipitation influence smoothed out with depth since soil water isotopes
3 approached groundwater signatures at 0.5 m soil depth.

4 **4.2.2 Seasonal isotope soil profiling**

5 Soil water was enriched in summer due to evaporation during warmer and drier periods
6 (Darling, 2004). The depth to which soil water isotopes are significantly affected by
7 evaporation is rarely more than 1–2 m below ground, and often less under temperate climates
8 (Darling, 2004). In contrast, winter profiles exhibited somewhat greater standard deviations in
9 comparison to summer isotopic soil profiles, indicative for wetter soils (Fig. 6, lower panels)
10 and shorter residence times (Thomas et al., 2013). Generally, deeper soil water isotope values
11 were relatively constant through time and space. Similar findings were made by Foerstel et al.
12 (1991) on a sandy soil at Juelich, western Germany and by McConville et al. (2001) under
13 predominately agriculturally used gley and till soils in Northern Ireland. Thomas et al. (2013)
14 likewise observed that soil water isotope samples from shallow soils (≤ 30 cm) were
15 comparable to precipitation isotopic composition, while samples from intermediate soils (40–
16 100 cm) plot near the groundwater average for a forested catchment located in central
17 Pennsylvania, USA. Furthermore, Tang and Feng (2001) showed for a sandy loam soil
18 sampling site in New Hampshire (USA) that the influence of summer precipitation decreased
19 with increasing depth, and soil at 0.5 m can only receive water from large storms. For summer
20 soil profiles under arable land, precipitation input signals similarly decreased with depth (Fig.
21 6, upper left panel). Generally, the replacement of old soil water with new infiltrating water is
22 dependent on the frequency and intensity of precipitation and the soil texture, structure,
23 wetness, and water potential of the soil (Li et al., 2007; Tang and Feng, 2001). It is usually
24 more efficient in a wet year than in a dry year (Tang and Feng, 2001). As a result of soil water
25 recharge near the surface, the amount of percolating water decreases with depth and
26 consequently, deeper soil layers have less chance to obtain new water (Tang and Feng, 2001).
27 Summer and winter profiles show higher water contents in the upper 0.2 m than further down
28 (Fig. 6, lower panels). Furthermore, in the growing season, the percolation depth is
29 additionally limited by plants' transpiration (Tang and Feng, 2001). For the Schwingbach
30 catchment we conclude that the influence of new percolating soil water decreased with depth
31 as no remarkable seasonality in soil isotopic signatures was obvious at >0.9 m and constant
32 values were observed through space and time.

1 **4.3 Linkages between water cycle components**

2 In general, stream water isotopic time series of the Vollnkirchener Bach and Schwingbach
3 showed (with few exceptions) little deflections through time and, consequently, provided little
4 insight into time and source-components connectivity. Schürch et al. (2003) likewise
5 observed damped river water isotopic signatures as compared with precipitation isotopic
6 signatures for sampling points of the “Swiss National Network for the Observation of
7 Isotopes in the Water Cycle”. For larger rivers like the Elbe at Torgau in eastern Germany
8 seasonal isotopic composition varied with an amplitude of 1.5‰ in $\delta^{18}\text{O}$ (Darling, 2004).

9 As described above, MTT calculations did not provide meaningful results. The failure of the
10 MTT estimations is mainly attributed to the little variation in stream water isotopic signatures.
11 Just as in the here presented results, Klaus et al. (2015) had difficulties to apply traditional
12 methods of isotope hydrology (MTT estimation, hydrograph separation) to their dataset due to
13 the lack of temporal isotopic variation in stream water of a forested low-mountainous
14 catchment in South Carolina (USA). Furthermore, stable water isotopes can only be utilised
15 for estimations of younger water (<5 years) (McGuire et al., 2005; Stewart et al., 2010),
16 suggesting that transit times in the Schwingbach catchment are longer than the range used for
17 stable water isotopes.

18 Due to isotopic similarities of stream and groundwater, we assume that groundwater
19 predominantly feeds baseflow. Even during peak flow occurring in January 2012, December
20 to April or May 2013, rainfall input did not play a major role for stream water isotopic
21 composition although fast rainfall-runoff behaviours were observed by Orłowski et al. (2014).
22 Same observations were made by Jin et al. (2010) for the Red Canyon Creek watershed
23 (Wyoming, USA), indicating good hydraulic connection between surface water and shallow
24 groundwater and by Klaus et al. (2015) for a low-mountainous forested watershed in South
25 Carolina (USA), comparable to the Schwingbach catchment. The damped groundwater
26 isotopic signatures, which likewise showed little variation through time, rather seemed to be a
27 mixture of former lighter precipitation events and snowmelt, since meltwater is known to be
28 depleted in stable isotopes as compared to the annual mean of precipitation or groundwater
29 (Rohde, 1998). However, one should be aware that differences in the snow sampling method
30 (new snow, snow pit layers, meltwater) can affect the isotopic composition (Penna et al.,
31 2014; Taylor et al., 2001). As groundwater at the observed piezometers in the Vollnkirchener
32 subcatchment is shallow (Orłowski et al., 2014), the snowmelt signal is allowed to move

1 rapidly through the soil. Pulses of snowmelt water causing a depletion in spring and early
2 summer was also observed by other studies (Darling, 2004; Kortelainen and Karhu, 2004).
3 We therefore assume that groundwater is mainly recharged throughout the winter. Generally,
4 less than 5 to 25% of precipitation infiltrates to the groundwater table in temperate climates;
5 the rest is lost to runoff, evaporation from soils, and transpiration by vegetation (Clark and
6 Fritz, 1997a). During spring runoff when soils are saturated, temperatures are low, and
7 vegetation is inactive, recharge rates are generally highest. In contrast, recharge is very low
8 during summer when most precipitation is transpired back to the atmosphere (Clark and Fritz,
9 1997a). Similarly, O'Driscoll et al. (2005) showed that summer precipitation does not
10 significantly contribute to recharge in the Spring Creek watershed of central Pennsylvania
11 (USA) since $\delta^{18}\text{O}$ values in summer precipitation were enriched compared to mean annual
12 groundwater composition.

13 Further, Orłowski et al. (2014) showed that influent and effluent conditions occurred
14 simultaneously at different stream sections of the Vollnkirchener Bach affecting stream and
15 groundwater isotopic compositions, equally. Since groundwater head levels in the
16 Vollnkirchener Bach subcatchment closely followed stream runoff-dynamics and responded
17 to stormflow events with rising head levels (Fig. 8), we conclude that bidirectional water
18 exchange between the groundwater body and the Vollnkirchener Bach occurred. Our network
19 map supported this assumption (Fig. 9) as surface water samplings points plotted close to
20 groundwater sampling points (especially to the sampling points under the meadow and along
21 the stream). However, both water compartments differed significantly from rainfall isotopic
22 signatures (Table 1). These divergent isotopic signatures but the prompt reaction of the
23 groundwater body to rainfall-runoff events indicate that 'old' groundwater can be released
24 during very short times (Kirchner, 2003). Thus, our catchment showed double water paradox
25 behaviour as described earlier by Kirchner (2003) as the fast releasing of very old water with
26 little variation in tracer concentration. This paradox behaviour could likewise be a reason for
27 the failure of the MTT estimation. Just by comparing mean precipitation ($\delta^{18}\text{O} = -6.2 \pm 3.1$),
28 stream (e.g. $\delta^{18}\text{O} = -8.4 \pm 0.4$ for the Vollnkirchener Bach), and groundwater isotopic
29 signatures ($\delta^{18}\text{O} = -8.2 \pm 0.4$ for the meadow) (Table 1), it is obvious that simple mixing
30 calculations do not work either.

31 Nevertheless, to still estimate groundwater ages in the Vollnkirchener Bach subcatchment, we
32 established a hydrological model. Our model results suggest that the main groundwater flow

1 direction is towards the stream and the quantity of flowing water is highest near the stream
2 (Fig. 10). This further supports the assumption that stream water is mainly fed by
3 groundwater. Moreover, the simulation underlines the conclusion that the groundwater body
4 and stream water are disconnected from the precipitation cycle, since only 13.3% of cells
5 contained water with an age <1 year. The results of the model reveal a spatially highly
6 heterogeneous age distribution of groundwater throughout the Vollnkirchener Bach
7 subcatchment. The age varies from about two days to more than 100 years with oldest water
8 near the stream. Thus, our model provides the opportunity to make use of stable water isotope
9 information along with climate, land use, and soil type data, in combination with a digital
10 elevation map to estimate residence times >5 years. Such long residence times could
11 previously only be determined via other tracers such as tritium (e.g. Michel (1992)). If stable
12 water isotope information is used alone, it is known to cause a truncation of stream residence
13 time distributions (Stewart et al., 2010). Moreover, our model facilitates the estimation of
14 spatially distributed groundwater ages, which opens up new opportunities to compare
15 groundwater ages from over a range of scales within catchments.

16 The observation that gaining and losing stream reaches occur simultaneously along the
17 Vollnkirchner Bach could similarly be supported by our model results. However, due to the
18 model assumption of a constant groundwater recharge over the course of a year, no
19 seasonality was simulated. Moreover, model results differ somewhat from the conceptual
20 model of Orłowski et al. (2014). This is due to the fact that the hydrological model only
21 estimates groundwater fluxes but not surface water fluxes. Moreover, no spatial differences in
22 soil properties of the groundwater layer were considered. Nevertheless, as shown by the
23 diverse ages of water in the stream cells and the assumption of spatially gaining conditions,
24 the model confirms that the stream contains water with different transit times. Therefore, the
25 stream water does not have a discrete age, but a distribution of ages due to variable flow paths
26 throughout the subcatchment (Stewart et al., 2010). Heidebüchel et al. (2012) proposed the
27 concept of the master transit time distribution that accounts for temporal variability of MTT.
28 Our model provides a different approach that considers spatial aspects of transit times and
29 gives a much deeper understanding of the groundwater-surface water connectivity across the
30 landscape than a classical MTT calculation could provide.

31 However, our semi-conceptual model approach has also some limitations. During model setup
32 a series of assumptions and simplifications were made to develop a realistic hydrologic model

1 without a severe loss in performance. Therefore, several parameters such as the depth of the
2 groundwater body are only rough estimations, while others like evapotranspiration are based
3 on simulations. Moreover, the groundwater body is highly simplified since e.g. properties of
4 the simulated aquifer are assumed to be constant over the subcatchment. However, the
5 complexity of the model is higher than in a simple one dimensional model (with only one cell
6 and one layer), which results in a better spatial resolution, but lower than in a fully distributed
7 variable saturated 3D model. In future models a more diverse groundwater body based on
8 small-scale measurements of aquifer parameters should be implemented. Especially data of
9 saturated hydraulic conductivity with high spatial resolution, as well as the implementation of
10 a temporal dynamic groundwater recharge could lead to an enhanced model performance.
11 Nevertheless, our hydrological model enables a good assessment of the groundwater age for
12 the Vollnkirchner Bach subcatchment and supports the assumption that surface and
13 groundwater are disconnected from precipitation.

14 **5 Conclusions**

15 Conducting a stable water isotope study in the Schwingbach catchment helped to identify
16 relationships between precipitation, stream, soil, and groundwater in a developed (managed)
17 catchment. The close isotopic link between groundwater and the streams revealed that
18 groundwater controls streamflow. Moreover, it could be shown that groundwater was
19 predominately recharged during winter but was decoupled from the annual precipitation
20 cycle. Even so streamflow and groundwater head levels promptly responded to precipitation
21 inputs, there was no obvious change in their isotopic composition due to rain events (old
22 water paradox behaviour). This was underlined by the fact that no remarkable seasonality in
23 soil isotopic signatures as interface between precipitation and groundwater was obvious at
24 >0.9 m and constant values were observed through space and time.

25 Nevertheless, the lack of temporal variation in stable isotope time series of stream and
26 groundwater (with few exceptions) limited the application of classical methods of isotope
27 hydrology, i.e. mean transit time estimations in the Schwingbach catchment. We therefore
28 setup a hydrological model with CMF to estimate groundwater ages and flow directions in the
29 Vollnkirchner Bach subcatchment. Our model result supported the finding that the water in
30 the catchment is >5 years (on average 16 years) and that stream water is mainly fed by
31 groundwater. Our modelling approach was valuable to overcome the limitations of MTT
32 calculations with traditional methods and/or models. Thus, our dual isotope study in

1 combination with a hydrological model approach was valuable for determining the
2 connectivity and disconnectivity between different water cycle components.

3

4 **Acknowledgements**

5 The first author acknowledges financial support by the Friedrich-Ebert-Stiftung (Bonn, DE).
6 Furthermore, this work was supported by the Deutsche Forschungsgemeinschaft under Grant
7 BR2238/10-1. Thanks also to the student assistants, BSc. and MSc. students for their help
8 during field sampling campaigns and hydrological modelling. In this regard we like to
9 acknowledge especially Julia Mechsner, Julia Klöber, and Judith Henkel. We thank Dr.
10 Christine Stumpp from the Helmholtz Zentrum München for providing us the isotope data
11 from GNIP station Koblenz.

12

1 **References**

- 2 Aggarwal, P. K., Gat, J. R. and Froehlich, K. F., Eds.: *Isotopes in the Water Cycle: Past,*
3 *Present and Future of a Developing Science*, Springer, Dordrecht, Netherlands., 2007.
- 4 Alaoui, A., Caduff, U., Gerke, H. H. and Weingartner, R.: *Preferential Flow Effects on*
5 *Infiltration and Runoff in Grassland and Forest Soils*, *Vadose Zone J.*, 10(1), 367,
6 doi:10.2136/vzj2010.0076, 2011.
- 7 Allan, J. D.: *Landscapes and Riverscapes: The Influence of Land Use on Stream Ecosystems*,
8 *Annu. Rev. Ecol. Evol. Syst.*, 35, 257–284, 2004.
- 9 Araguás-Araguás, L., Froehlich, K. and Rozanski, K.: *Deuterium and oxygen-18 isotope*
10 *composition of precipitation and atmospheric moisture*, *Hydrol. Process.*, 14(8), 1341–1355,
11 2000.
- 12 Argiriou, A. A. and Lykoudis, S.: *Isotopic composition of precipitation in Greece*, *J. Hydrol.*,
13 327(3–4), 486–495, doi:10.1016/j.jhydrol.2005.11.053, 2006.
- 14 Barnes, C. J. and Allison, G. B.: *Tracing of water movement in the unsaturated zone using*
15 *stable isotopes of hydrogen and oxygen*, *J. Hydrol.*, 100(1–3), 143–176, doi:10.1016/0022-
16 1694(88)90184-9, 1988.
- 17 Barthold, F. K., Tyralla, C., Schneider, K., Vaché, K. B., Frede, H.-G. and Breuer, L.: *How*
18 *many tracers do we need for end member mixing analysis (EMMA)? A sensitivity analysis*,
19 *Water Resour. Res.*, 47(8), doi:10.1029/2011WR010604, 2011.
- 20 Birkel, C., Dunn, S. M., Tetzlaff, D. and Soulsby, C.: *Assessing the value of high-resolution*
21 *isotope tracer data in the stepwise development of a lumped conceptual rainfall–runoff model*,
22 *Hydrol. Process.*, 24(16), 2335–2348, doi:10.1002/hyp.7763, 2010.
- 23 Blasch, K. W. and Bryson, J. R.: *Distinguishing Sources of Ground Water Recharge by Using*
24 $\delta^2\text{H}$ and $\delta^{18}\text{O}$, *Ground Water*, 45(3), 294–308, doi:10.1111/j.1745-6584.2006.00289.x, 2007.
- 25 Bony, S., Risi, C. and Vimeux, F.: *Influence of convective processes on the isotopic*
26 *composition ($\delta^{18}\text{O}$ and δD) of precipitation and water vapor in the tropics: 1. Radiative-*
27 *convective equilibrium and Tropical Ocean–Global Atmosphere–Coupled Ocean–Atmosphere*
28 *Response Experiment (TOGA-COARE) simulations*, *J. Geophys. Res. Atmospheres*,
29 113(D19), D19305, doi:10.1029/2008JD009942, 2008.
- 30 Botter, G., Bertuzzo, E. and Rinaldo, A.: *Transport in the hydrologic response: Travel time*
31 *distributions, soil moisture dynamics, and the old water paradox*, *Water Resour. Res.*, 46(3),
32 W03514, doi:10.1029/2009WR008371, 2010.
- 33 Bowen, G. J. and Wilkinson, B.: *Spatial distribution of $\delta^{18}\text{O}$ in meteoric precipitation*,
34 *Geology*, 30(4), 315–318, doi:10.1130/0091-7613(2002)030<0315:SDOOIM>2.0.CO;2,
35 2002.

- 1 Brodersen, C., Pohl, S., Lindenlaub, M., Leibundgut, C. and Wilpert, K. v: Influence of
2 vegetation structure on isotope content of throughfall and soil water, *Hydrol. Process.*, 14(8),
3 1439–1448, doi:10.1002/1099-1085(20000615)14:8<1439::AID-HYP985>3.0.CO;2-3, 2000.
- 4 Burger, H. M. and Seiler, K. P.: Evaporation from soil water under humid climate conditions
5 and its impact on deuterium and ¹⁸O concentrations in groundwater., edited by International
6 Atomic Energy Agency, pp. 674–678, International Atomic Energy Agency, Vienna, Austria.,
7 1992.
- 8 Buttle, J. M.: Isotope hydrograph separations and rapid delivery of pre-event water from
9 drainage basins, *Prog. Phys. Geogr.*, 18(1), 16–41, doi:10.1177/030913339401800102, 1994.
- 10 Buttle, J. M.: Isotope Hydrograph Separation of Runoff Sources, in *Encyclopedia of*
11 *Hydrological Sciences*, edited by M. G. Anderson, p. 10:116, John Wiley & Sons, Ltd,
12 Chichester, Great Britain, 2006.
- 13 Buttle, J. M. and McDonald, D. J.: Coupled vertical and lateral preferential flow on a forested
14 slope, *Water Resour. Res.*, 38(5), 18–1, doi:10.1029/2001WR000773, 2002.
- 15 Choi, S.-H.: Characteristics of hydrogeologic units of groundwater resources in the Republic
16 of Korea, in *Engineering Geology and the Environment*, vol. 4, edited by P. G. Marinos, G. C.
17 Koukis, G. C. Tsiambaos, and G. C. Stournaras, pp. 1219–1224, CRC Press, Florida, USA.,
18 1997.
- 19 Clark, I. D. and Fritz, P.: Groundwater, in *Environmental Isotopes in Hydrogeology*, p.80,
20 CRC Press, Florida, FL, USA., 1997a.
- 21 Clark, I. D. and Fritz, P.: Methods for Field Sampling, in *Environmental Isotopes in*
22 *Hydrogeology*, p. 283, CRC Press, Florida, FL, USA., 1997b.
- 23 Clark, I. D. and Fritz, P.: The Environmental Isotopes, in *Environmental Isotopes in*
24 *Hydrogeology*, pp. 2–34, CRC Press, Florida, FL, USA., 1997c.
- 25 Cooper, L. W.: Isotopic Fractionation in Snow Cover, in *Isotope Tracers in Catchment*
26 *Hydrology*, edited by C. Kendall and J. J. McDonnell, pp. 119–136, Elsevier, Amsterdam,
27 Netherlands., 1998.
- 28 Craig, H.: Isotopic Variations in Meteoric Waters, *Science*, 133(3465), 1702–1703,
29 doi:10.1126/science.133.3465.1702, 1961a.
- 30 Craig, H.: Standard for reporting concentrations of deuterium and oxygen-18 in natural
31 waters, *Science*, 133(3467), 1833, 1961b.
- 32 Csardi, G. and Nepusz, T.: The igraph software package for complex network research,
33 *Complex Systems* 1695. [online] Available from: <http://igraph.sf.net> (Accessed 24 December
34 2015), 2006.
- 35 Dansgaard, W.: Stable isotopes in precipitation, *Tellus*, 16(4), 436–468, doi:10.1111/j.2153-
36 3490.1964.tb00181.x, 1964.

- 1 Darling, W. G.: Hydrological factors in the interpretation of stable isotopic proxy data present
2 and past: a European perspective, *Quat. Sci. Rev.*, 23(7–8), 743–770,
3 doi:10.1016/j.quascirev.2003.06.016, 2004.
- 4 Day, T. J.: On the precision of salt dilution gauging, *J. Hydrol.*, 31(3–4), 293–306,
5 doi:10.1016/0022-1694(76)90130-X, 1976.
- 6 DWD: Deutscher Wetterdienst - Wetter und Klima, Bundesministerium für Verkehr und
7 digitale Infrastruktur, [online] Available from: <http://dwd.de/> (Accessed 17 February 2014),
8 2014.
- 9 Eijkelkamp: RBC flumes, [online] Available from:
10 [http://en.eijkelkamp.com/products/water/hydrological-research/water-discharge-](http://en.eijkelkamp.com/products/water/hydrological-research/water-discharge-measurements/rbc-flumes.htm)
11 [measurements/rbc-flumes.htm](http://en.eijkelkamp.com/products/water/hydrological-research/water-discharge-measurements/rbc-flumes.htm) (Accessed 13 January 2014), 2014.
- 12 Foerstel, H., Frinken, J., Huetzen, H., Lembrich, D. and Puetz, T.: Application of H₂¹⁸O as a
13 tracer of water flow in soil, *International Atomic Energy Agency, Vienna, Austria*, 1991.
- 14 Froehlich, K., Gibson, J. J. and Aggarwal, P. K.: Deuterium excess in precipitation and its
15 climatological significance, in *Study of Environmental Changes Using Isotope Techniques*,
16 pp. 54–65, C&S Paper Series 13/P, International Atomic Energy Agency, Vienna, Austria.,
17 2002.
- 18 Garvelmann, J., Kuells, C. and Weiler, M.: A porewater-based stable isotope approach for the
19 investigation of subsurface hydrological processes, *Hydrol. Earth Syst. Sci.*, 16(2), 631–640,
20 doi:10.5194/hess-16-631-2012, 2012.
- 21 Gat, J. R.: Oxygen and Hydrogen Isotopes in the Hydrologic Cycle, *Annu. Rev. Earth Planet.*
22 *Sci.*, 24(1), 225–262, doi:10.1146/annurev.earth.24.1.225, 1996.
- 23 Gat, J., R., Mook, W. G. and Meijer, H. A. J.: Environmental isotopes in the hydrological
24 cycle: Principles and Applications, edited by W. G. Mook, International Hydrological
25 Programme; United Nations Educational, Scientific and Cultural Organization and
26 International Atomic Energy Agency, Paris, France., 2001.
- 27 Gehrels, J. C., Peeters, J. E. M., de Vries, J. J. and Dekkers, M.: The mechanism of soil water
28 movement as inferred from ¹⁸O stable isotope studies, *Hydrol. Sci. J.*, 43(4), 579–594,
29 doi:10.1080/02626669809492154, 1998.
- 30 Genereux, D. P. and Hooper, R. P.: Oxygen and Hydrogen Isotopes in Rainfall-Runoff
31 Studies, in *Isotope Tracers in Catchment Hydrology*, edited by C. Kendall and J. J.
32 McDonnell, pp. 319–346, Elsevier, Amsterdam, Netherlands., 1998.
- 33 Goller, R., Wilcke, W., Leng, M. J., Tobschall, H. J., Wagner, K., Valarezo, C. and Zech, W.:
34 Tracing water paths through small catchments under a tropical montane rain forest in south
35 Ecuador by an oxygen isotope approach, *J. Hydrol.*, 308(1–4), 67–80,
36 doi:10.1016/j.jhydrol.2004.10.022, 2005.
- 37 Gonfiantini, R., Fröhlich, K., Araguás-Araguás, L. and Rozanski, K.: Isotopes in
38 Groundwater Hydrology, in *Isotope Tracers in Catchment Hydrology*, edited by C. Kendall
39 and J. J. McDonnell, pp. 203–246, Elsevier, Amsterdam, Netherlands., 1998.

- 1 Goni, I. B.: Tracing stable isotope values from meteoric water to groundwater in the
2 southwestern part of the Chad basin, *Hydrogeol. J.*, 14(5), 742–752, doi:10.1007/s10040-005-
3 0469-y, 2006.
- 4 Gordon, L. J., Finlayson, C. M. and Falkenmark, M.: Managing water in agriculture for food
5 production and other ecosystem services, *Agric. Water Manag.*, 97(4), 512–519,
6 doi:10.1016/j.agwat.2009.03.017, 2010.
- 7 Heidebüchel, I., Troch, P. A., Lyon, S. W. and Weiler, M.: The master transit time distribution
8 of variable flow systems, *Water Resour. Res.*, 48(6), W06520, doi:10.1029/2011WR011293,
9 2012.
- 10 Hoeg, S., Uhlenbrook, S. and Leibundgut, C.: Hydrograph separation in a mountainous
11 catchment — combining hydrochemical and isotopic tracers, *Hydrol. Process.*, 14(7), 1199–
12 1216, doi:10.1002/(SICI)1099-1085(200005)14:7<1199::AID-HYP35>3.0.CO;2-K, 2000.
- 13 Hollander, M., Wolfe, D. A. and Chicken, E.: *Nonparametric Statistical Methods*, John Wiley
14 & Sons, New York, NY, USA., 2013.
- 15 Hsieh, J. C. C., Chadwick, O. A., Kelly, E. F. and Savin, S. M.: Oxygen isotopic composition
16 of soil water: quantifying evaporation and transpiration, *Geoderma*, 82(1-3), 269–293,
17 doi:10.1016/S0016-7061(97)00105-5, 1998.
- 18 IAEA: International Atomic Energy Agency: Water Resources Programme – Global Network
19 of Isotopes in Precipitation, [online] Available from: [http://www-](http://www-naweb.iaea.org/naweb/ih/IHS_resources_gnip.html)
20 [naweb.iaea.org/naweb/ih/IHS_resources_gnip.html](http://www-naweb.iaea.org/naweb/ih/IHS_resources_gnip.html) (Accessed 11 August 2014), 2014.
- 21 Ivkovic, K. M.: A top–down approach to characterise aquifer–river interaction processes, *J.*
22 *Hydrol.*, 365(3–4), 145–155, doi:10.1016/j.jhydrol.2008.11.021, 2009.
- 23 Jin, L., Siegel, D. I., Lautz, L. K., Mitchell, M. J., Dahms, D. E. and Mayer, B.: Calcite
24 precipitation driven by the common ion effect during groundwater–surface-water mixing: A
25 potentially common process in streams with geologic settings containing gypsum, *Geol. Soc.*
26 *Am. Bull.*, 122(7/8), B30011.1, doi:10.1130/B30011.1, 2010.
- 27 Jin, L., Siegel, D. I., Lautz, L. K. and Lu, Z.: Identifying streamflow sources during spring
28 snowmelt using water chemistry and isotopic composition in semi-arid mountain streams, *J.*
29 *Hydrol.*, 470–471, 289–301, doi:10.1016/j.jhydrol.2012.09.009, 2012.
- 30 Jolliffe, I. T.: *Principal Component Analysis*, 2nd ed., Springer Science & Business Media,
31 New York, NY, USA., 2002.
- 32 Jouzel, J., Alley, R. B., Cuffey, K. M., Dansgaard, W., Grootes, P., Hoffmann, G., Johnsen, S.
33 J., Koster, R. D., Peel, D., Shuman, C. A., Stievenard, M., Stuiver, M. and White, J.: Validity
34 of the temperature reconstruction from water isotopes in ice cores, *J. Geophys. Res.*, 102,
35 26471–26487, doi:10.1029/97JC01283, 1997.
- 36 Kendall, C. and Caldwell, E. A.: Fundamentals of Isotope Geochemistry, in *Isotope Tracers in*
37 *Catchment Hydrology*, edited by C. Kendall and J. J. McDonnell, pp. 51–86, Elsevier,
38 Amsterdam, Netherlands., 1998.

- 1 Kendall, C. and Coplen, T. B.: Distribution of oxygen-18 and deuterium in river waters across
2 the United States, *Hydrol. Process.*, 15, 1363–1393, doi:10.1002/hyp.217, 2001.
- 3 Kirchner, J. W.: A double paradox in catchment hydrology and geochemistry, *Hydrol.*
4 *Process.*, 17(4), 871–874, doi:10.1002/hyp.5108, 2003.
- 5 Klapper, H.: *Historical Change of Large Alluvial Rivers: Western Europe*, edited by G. E.
6 Petts, H. Möller, and A. L. Roux, John Wiley and Sons Ltd., Chichester, Great Britain, 1990.
- 7 Klaus, J., McDonnell, J. J., Jackson, C. R., Du, E. and Griffiths, N. A.: Where does
8 streamwater come from in low-relief forested watersheds? A dual-isotope approach, *Hydrol.*
9 *Earth Syst. Sci.*, 19(1), 125–135, 2015.
- 10 Koeniger, P., Leibundgut, C. and Stichler, W.: Spatial and temporal characterisation of stable
11 isotopes in river water as indicators of groundwater contribution and confirmation of
12 modelling results; a study of the Weser river, Germany, *Isotopes Environ. Health Stud.*, 45(4),
13 289–302, doi:10.1080/10256010903356953, 2009.
- 14 Koivusalo, H., Karvonen, T. and Lepistö, A.: A quasi-three-dimensional model for predicting
15 rainfall-runoff processes in a forested catchment in Southern Finland, *Hydrol. Earth Syst.*
16 *Sci.*, 4(1), 65–78, doi:10.5194/hess-4-65-2000, 1999.
- 17 Kolaczyk, E. D.: *Statistical Analysis of Network Data with R*, Springer Science & Business
18 Media, New York, NY, USA., 2014.
- 19 Kortelainen, N. M. and Karhu, J. A.: Regional and seasonal trends in the oxygen and
20 hydrogen isotope ratios of Finnish groundwaters: a key for mean annual precipitation, *J.*
21 *Hydrol.*, 285(1–4), 143–157, doi:10.1016/j.jhydrol.2003.08.014, 2004.
- 22 Kraft, P., Vaché, K. B., Frede, H.-G. and Breuer, L.: CMF: A Hydrological Programming
23 Language Extension For Integrated Catchment Models, *Environ. Model. Softw.*, 26(6), 828–
24 830, doi:10.1016/j.envsoft.2010.12.009, 2011.
- 25 Ladouche, B., Probst, A., Viville, D., Idir, S., Baqu'e, D., Loubet, M., Probst, J. L. and
26 Bariac, T.: Hydrograph separation using isotopic, chemical and hydrological approaches
27 (Strengbach catchment, France), *J. Hydrol.*, 242(3), 255–274, 2001.
- 28 Lai, C.-T. and Ehleringer, J. R.: Deuterium excess reveals diurnal sources of water vapor in
29 forest air, *Oecologia*, 165(1), 213–223, doi:10.1007/s00442-010-1721-2, 2011.
- 30 Lauer, F., Frede, H.-G. and Breuer, L.: Uncertainty assessment of quantifying spatially
31 concentrated groundwater discharge to small streams by distributed temperature sensing,
32 *Water Resour. Res.*, 49(1), 400–407, doi:10.1029/2012WR012537, 2013.
- 33 Leen, J. B., Berman, E. S. F., Liebson, L. and Gupta, M.: Spectral contaminant identifier for
34 off-axis integrated cavity output spectroscopy measurements of liquid water isotopes, *Rev.*
35 *Sci. Instrum.*, 83(4), doi:10.1063/1.4704843, 2012.
- 36 LGR: Los Gatos Research, Greenhouse Gas, isotope and trace gas analyzers, [online]
37 Available from: <http://www.lgrinc.com/> (Accessed 5 February 2013), 2013.

- 1 Liebminger, A., Haberhauer, G., Papesch, W., Heiss, G. and others: Footprints of climate in
2 groundwater and precipitation, *Hydrol. Earth Syst. Sci.*, 11(2), 785–791, doi:10.5194/hess-11-
3 785-2007, 2007.
- 4 Li, F., Song, X., Tang, C., Liu, C., Yu, J. and Zhang, W.: Tracing infiltration and recharge
5 using stable isotope in Taihang Mt., North China, *Environ. Geol.*, 53(3), 687–696,
6 doi:10.1007/s00254-007-0683-0, 2007.
- 7 Maloszewski, P. and Zuber, A.: Lumped parameter models for interpretation of
8 environmental tracer data, in *Manual on Mathematical Models in Isotope Hydrogeology*,
9 International Atomic Energy Agency, Vienna, Austria., 1996.
- 10 Maloszewski, P. and Zuber, A.: Manual on lumped parameter models used for the
11 interpretation of environmental tracer data in groundwaters, in *Use of isotopes for analyses of*
12 *flow and transport dynamics in groundwater systems*, p. 50, International Atomic Energy
13 Agency, Vienna, Austria., 2002.
- 14 Maule, C. P., Chanasyk, D. S. and Muehlenbachs, K.: Isotopic determination of snow-water
15 contribution to soil water and groundwater, *J. Hydrol.*, 155(1-2), 73–91, doi:10.1016/0022-
16 1694(94)90159-7, 1994.
- 17 Mazor, E.: Part I. Physical and Geological Concepts, 2. Basic Hydrological Concepts, in
18 *Chemical and Isotopic Groundwater Hydrology*, pp. 15–48, CRC Press, Boca Raton, Florida,
19 USA., 2003.
- 20 McConville, C., Kalin, R. m., Johnston, H. and McNeill, G. w.: Evaluation of Recharge in a
21 Small Temperate Catchment Using Natural and Applied $\delta^{18}\text{O}$ Profiles in the Unsaturated
22 Zone, *Ground Water*, 39(4), 616–623, doi:10.1111/j.1745-6584.2001.tb02349.x, 2001.
- 23 McDonnell, J. J., Sivapalan, M., Vaché, K., Dunn, S., Grant, G., Haggerty, R., Hinz, C.,
24 Hooper, R., Kirchner, J., Roderick, M. L. and others: Moving beyond heterogeneity and
25 process complexity: a new vision for watershed hydrology, *Water Resour. Res.*, 43(7),
26 W07301, 2007.
- 27 McGuire, K. ., DeWalle, D. . and Gburek, W. .: Evaluation of mean residence time in
28 subsurface waters using oxygen-18 fluctuations during drought conditions in the mid-
29 Appalachians, *J. Hydrol.*, 261(1–4), 132–149, doi:10.1016/S0022-1694(02)00006-9, 2002.
- 30 McGuire, K. J., McDonnell, J. J., Weiler, M., Kendall, C., McGlynn, B. L., Welker, J. M. and
31 Seibert, J.: The role of topography on catchment-scale water residence time, *Water Resour.*
32 *Res.*, 41(5), W05002, doi:10.1029/2004WR003657, 2005.
- 33 Michel, R. L.: Residence times in river basins as determined by analysis of long-term tritium
34 records, *J. Hydrol.*, 130(1), 367–378, doi:10.1016/0022-1694(92)90117-E, 1992.
- 35 Mook, W. G., Ed.: *Environmental Isotopes in the Hydrological Cycle: Principles and*
36 *Applications*, International Hydrological Programme; United Nations Educational, Scientific
37 and Cultural Organization and International Atomic Energy Agency, Paris, Vienna., 2001.

- 1 Mook, W. G., Groeneveld, D. J., Brouwn, A. E. and Ganswijk, A. J. van: Analysis of a run-
2 off hydrograph by means of natural ^{18}O , in *Isotope techniques in groundwater hydrology*, vol.
3 1, pp. 159–169, International Atomic Energy Agency, Vienna, Austria., 1974.
- 4 Moore, R. D.: Introduction to Salt Dilution Gauging for Streamflow Measurement: Part 1,
5 *Streamline Watershed Manag. Bull.*, 7(4), 20–23, 2004.
- 6 Munyaneza, O., Wenninger, J. and Uhlenbrook, S.: Identification of runoff generation
7 processes using hydrometric and tracer methods in a meso-scale catchment in Rwanda,
8 *Hydrol. Earth Syst. Sci.*, 16(7), 1991–2004, doi:10.5194/hess-16-1991-2012, 2012.
- 9 Neal, C. and Rosier, P. T. W.: Chemical studies of chloride and stable oxygen isotopes in two
10 conifer afforested and moorland sites in the British uplands, *J. Hydrol.*, 115(1–4), 269–283,
11 doi:10.1016/0022-1694(90)90209-G, 1990.
- 12 O’Driscoll, M., Clinton, S., Jefferson, A., Manda, A. and McMillan, S.: Urbanization Effects
13 on Watershed Hydrology and In-Stream Processes in the Southern United States, *Water*, 2(3),
14 605–648, doi:10.3390/w2030605, 2010.
- 15 O’Driscoll, M. A., DeWalle, D. R., McGuire, K. J. and Gburek, W. J.: Seasonal ^{18}O variations
16 and groundwater recharge for three landscape types in central Pennsylvania, USA, *J. Hydrol.*,
17 303(1–4), 108–124, doi:10.1016/j.jhydrol.2004.08.020, 2005.
- 18 Orłowski, N., Frede, H.-G., Brüggemann, N. and Breuer, L.: Validation and application of a
19 cryogenic vacuum extraction system for soil and plant water extraction for isotope analysis, *J.*
20 *Sens. Sens. Syst.*, 2(2), 179–193, doi:10.5194/jsss-2-179-2013, 2013.
- 21 Orłowski, N., Lauer, F., Kraft, P., Frede, H.-G. and Breuer, L.: Linking Spatial Patterns of
22 Groundwater Table Dynamics and Streamflow Generation Processes in a Small Developed
23 Catchment, *Water*, 6(10), 3085–3117, doi:10.3390/w6103085, 2014.
- 24 Penna, D., Ahmad, M., Birks, S. J., Bouchaou, L., Brenčič, M., Butt, S., Holko, L., Jeelani,
25 G., Martínez, D. E., Melikadze, G., Shanley, J. B., Sokratov, S. A., Stadnyk, T., Sugimoto, A.
26 and Vreča, P.: A new method of snowmelt sampling for water stable isotopes, *Hydrol.*
27 *Process.*, 28(22), 5637–5644, doi:10.1002/hyp.10273, 2014.
- 28 Phillips, D. L. and Gregg, J. W.: Source partitioning using stable isotopes: coping with too
29 many sources, *Oecologia*, 136(2), 261–269, doi:10.1007/s00442-003-1218-3, 2003.
- 30 Pierce, S. C., Kröger, R. and Pezeshki, R.: Managing Artificially Drained Low-Gradient
31 Agricultural Headwaters for Enhanced Ecosystem Functions, *Biology*, 1(3), 794–856,
32 doi:10.3390/biology1030794, 2012.
- 33 Price, K., Jackson, C. R. and Parker, A. J.: Variation of surficial soil hydraulic properties
34 across land uses in the southern Blue Ridge Mountains, North Carolina, USA, *J. Hydrol.*,
35 383(3–4), 256–268, doi:10.1016/j.jhydrol.2009.12.041, 2010.
- 36 Qu, Y. and Duffy, C. J.: A semidiscrete finite volume formulation for multiprocess watershed
37 simulation, *Water Resour. Res.*, 43(8), W08419, doi:10.1029/2006WR005752, 2007.

- 1 Rinaldo, A., Benettin, P., Harman, C. J., Hrachowitz, M., McGuire, K. J., van der Velde, Y.,
2 Bertuzzo, E. and Botter, G.: Storage selection functions: A coherent framework for
3 quantifying how catchments store and release water and solutes, *Water Resour. Res.*, 51(6),
4 4840–4847, doi:10.1002/2015WR017273, 2015.
- 5 Risi, C., Bony, S., Vimeux, F., Descroix, L., Ibrahim, B., Lebreton, E., Mamadou, I. and
6 Sultan, B.: What controls the isotopic composition of the African monsoon precipitation?
7 Insights from event-based precipitation collected during the 2006 AMMA field campaign,
8 *Geophys. Res. Lett.*, 35(24), L24808, doi:10.1029/2008GL035920, 2008.
- 9 Rockström, J., Falkenmark, M., Allan, T., Folke, C., Gordon, L., Jägerskog, A., Kummu, M.,
10 Lannerstad, M., Meybeck, M., Molden, D., Postel, S., Savenije, H. h. g., Svedin, U., Turton,
11 A. and Varis, O.: The unfolding water drama in the Anthropocene: towards a resilience-based
12 perspective on water for global sustainability, *Ecohydrol.*, 7(5), 1249–1261,
13 doi:10.1002/eco.1562, 2014.
- 14 Rodgers, P., Soulsby, C. and Waldron, S.: Stable isotope tracers as diagnostic tools in
15 upscaling flow path understanding and residence time estimates in a mountainous mesoscale
16 catchment, *Hydrol. Process.*, 19(11), 2291–2307, doi:10.1002/hyp.5677, 2005a.
- 17 Rodgers, P., Soulsby, C., Waldron, S. and Tetzlaff, D.: Using stable isotope tracers to assess
18 hydrological flow paths, residence times and landscape influences in a nested mesoscale
19 catchment, *Hydrol. Earth Syst. Sci.*, 9(3), 139–155, 2005b.
- 20 Rohde, A.: Snowmelt-Dominated Systems, in *Isotope Tracers in Catchment Hydrology*,
21 edited by C. Kendall and J. J. McDonnell, pp. 391–433, Elsevier, Amsterdam, Netherlands.,
22 1998.
- 23 Rothfuss, Y., Biron, P., Braud, I., Canale, L., Durand, J.-L., Gaudet, J.-P., Richard, P.,
24 Vauclin, M. and Bariac, T.: Partitioning evapotranspiration fluxes into soil evaporation and
25 plant transpiration using water stable isotopes under controlled conditions, *Hydrol. Process.*,
26 24(22), 3177–3194, doi:10.1002/hyp.7743, 2010.
- 27 Rothfuss, Y., Braud, I., Le Moine, N., Biron, P., Durand, J.-L., Vauclin, M. and Bariac, T.:
28 Factors controlling the isotopic partitioning between soil evaporation and plant transpiration:
29 Assessment using a multi-objective calibration of SiSPAT-Isotope under controlled
30 conditions, *J. Hydrol.*, 442-443, 75–88, doi:10.1016/j.jhydrol.2012.03.041, 2012.
- 31 Rozanski, K., Sonntag, C. and Münnich, K. O.: Factors controlling stable isotope composition
32 of European precipitation, *Tellus*, 34(2), 142–150, doi:10.1111/j.2153-3490.1982.tb01801.x,
33 1982.
- 34 Rozanski, K., Araguás-Araguás, L. and Gonfiantini, R.: Isotopic Patterns in Modern Global
35 Precipitation, in *Climate Change in Continental Isotopic Records*, edited by P. K. Swart, K. C.
36 Lohmann, J. Mckenzie, and S. Savin, pp. 1–36, American Geophysical Union, Washington,
37 D. C., US. [online] Available from:
38 <http://onlinelibrary.wiley.com/doi/10.1029/GM078p0001/summary> (Accessed 13 August
39 2014), 1993.
- 40 Rozanski, K., Froehlich, K. and Mook, W. G.: in *Environmental isotopes in the hydrological*
41 *cycle: Principles and Applications*, vol. 3, International Hydrological Programme; United

- 1 Nations Educational, Scientific and Cultural Organization and International Atomic Energy
2 Agency, Paris, Vienna., 2001.
- 3 Schultz, N. M., Griffis, T. J., Lee, X. and Baker, J. M.: Identification and correction of
4 spectral contamination in $^2\text{H}/^1\text{H}$ and $^{18}\text{O}/^{16}\text{O}$ measured in leaf, stem, and soil water, *Rapid*
5 *Commun. Mass Spectrom.*, 25(21), 3360–3368, doi:10.1002/rcm.5236, 2011.
- 6 Schürch, M., Kozel, R., Schotterer, U. and Tripet, J.-P.: Observation of isotopes in the water
7 cycle—the Swiss National Network (NISOT), *Environ. Geol.*, 45(1), 1–11,
8 doi:10.1007/s00254-003-0843-9, 2003.
- 9 Sklash, M. G.: Environmental isotope studies of storm and snowmelt runoff generation, in
10 *Process studies in hillslope hydrology*, edited by M. G. Anderson, pp. 410–435, Wiley, New
11 York, NY, USA., 1990.
- 12 Sklash, M. G. and Farvolden, R. N.: The Role Of Groundwater In Storm Runoff, in
13 *Developments in Water Science*, vol. 12, edited by W. B. and D. A. Stephenson, pp. 45–65,
14 Elsevier. [online] Available from:
15 <http://www.sciencedirect.com/science/article/pii/S0167564809700097> (Accessed 8 October
16 2015), 1979.
- 17 Song, X., Wang, P., Yu, J., Liu, X., Liu, J. and Yuan, R.: Relationships between precipitation,
18 soil water and groundwater at Chongling catchment with the typical vegetation cover in the
19 Taihang mountainous region, China, *Environ. Earth Sci.*, 62(4), 787–796,
20 doi:10.1007/s12665-010-0566-7, 2011.
- 21 Stewart, M. K., Morgenstern, U. and McDonnell, J. J.: Truncation of stream residence time:
22 how the use of stable isotopes has skewed our concept of streamwater age and origin, *Hydrol.*
23 *Process.*, 24(12), 1646–1659, doi:10.1002/hyp.7576, 2010.
- 24 Stumpp, C., Klaus, J. and Stichler, W.: Analysis of long-term stable isotopic composition in
25 German precipitation, *J. Hydrol.*, 517, 351–361, doi:10.1016/j.jhydrol.2014.05.034, 2014.
- 26 Tang, K. and Feng, X.: The effect of soil hydrology on the oxygen and hydrogen isotopic
27 compositions of plants' source water, *Earth Planet. Sci. Lett.*, 185(3-4), 355–367, 2001.
- 28 Taylor, S., Feng, X., Kirchner, J. W., Osterhuber, R., Klaue, B. and Renshaw, C. E.: Isotopic
29 evolution of a seasonal snowpack and its melt, *Water Resour. Res.*, 37(3), 759–769,
30 doi:10.1029/2000WR900341, 2001.
- 31 Thomas, E. M., Lin, H., Duffy, C. J., Sullivan, P. L., Holmes, G. H., Brantley, S. L. and Jin,
32 L.: Spatiotemporal Patterns of Water Stable Isotope Compositions at the Shale Hills Critical
33 Zone Observatory: Linkages to Subsurface Hydrologic Processes, *Vadose Zone J.*, 12(4), 0,
34 doi:10.2136/vzj2013.01.0029, 2013.
- 35 Timbe, E., Windhorst, D., Crespo, P., Frede, H.-G., Feyen, J. and Breuer, L.: Understanding
36 uncertainties when inferring mean transit times of water through tracer-based lumped-
37 parameter models in Andean tropical montane cloud forest catchments, *Hydrol. Earth Syst.*
38 *Sci.*, 18(4), 1503–1523, doi:10.5194/hess-18-1503-2014, 2014.

- 1 UNEP: United Nations Environment Programme: Global Environment Outlook 3: Past,
2 Present and Future Perspectives, Earthscan Publications Ltd, London, United Kingdom.,
3 2002.
- 4 Wallis, W. D.: A Beginner's Guide to Graph Theory, Birkhäuser Boston, Boston, MA, USA.,
5 2007.
- 6 Wang, X. F. and Yakir, D.: Using stable isotopes of water in evapotranspiration studies,
7 *Hydrol. Process.*, 14(8), 1407–1421, doi:10.1002/1099-1085(20000615)14:8<1407::AID-
8 HYP992>3.0.CO;2-K, 2000.
- 9 Wassenaar, L. I., Athanasopoulos, P. and Hendry, M. J.: Isotope hydrology of precipitation,
10 surface and ground waters in the Okanagan Valley, British Columbia, Canada, *J. Hydrol.*,
11 411(1–2), 37–48, doi:10.1016/j.jhydrol.2011.09.032, 2011.
- 12 Whitefield, P.: Chapter 3: Soil, in *Earth Care Manual: A Permaculture Handbook for Britain
13 & Other Temperate Climates*, pp. 39–66, Permanent Publications, East Meon, UK., 2004.
- 14 Windhorst, D., Waltz, T., Timbe, E., Frede, H.-G. and Breuer, L.: Impact of elevation and
15 weather patterns on the isotopic composition of precipitation in a tropical montane rainforest,
16 *Hydrol. Earth Syst. Sci.*, 17(1), 409–419, doi:10.5194/hess-17-409-2013, 2013.
- 17 Windhorst, D., Kraft, P., Timbe, E., Frede, H.-G. and Breuer, L.: Stable water isotope tracing
18 through hydrological models for disentangling runoff generation processes at the hillslope
19 scale, *Hydrol. Earth Syst. Sci.*, 18(10), 4113–4127, doi:10.5194/hess-18-4113-2014, 2014.
- 20 Wu, J., Ding, Y., Ye, B., Yang, Q., Hou, D. and Xue, L.: Stable isotopes in precipitation in
21 Xilin River Basin, northern China and their implications, *Chin. Geogr. Sci.*, 22(5), 531–540,
22 doi:10.1007/s11769-012-0543-z, 2012.
- 23 Xia, Y.: Optimization and uncertainty estimates of WMO regression models for the
24 systematic bias adjustment of NLDAS precipitation in the United States, *J. Geophys. Res.*
25 *Atmospheres*, 111(D8), D08102, doi:10.1029/2005JD006188, 2006.
- 26 Yurtsever, Y.: *Worldwide survey of stable isotopes in precipitation*, International Atomic
27 Energy Agency, Vienna, Austria., 1975.
- 28 Zhang, Y., Shen, Y., Chen, Y. and Wang, Y.: Spatial characteristics of surface water and
29 groundwater using water stable isotope in the Tarim River Basin, northwestern China,
30 *Ecohydrol.*, 6(6), 1031–1039, doi:10.1002/eco.1416, 2013.
- 31 Zhao, L., Xiao, H., Zhou, J., Wang, L., Cheng, G., Zhou, M., Yin, L. and McCabe, M. F.:
32 Detailed assessment of isotope ratio infrared spectroscopy and isotope ratio mass
33 spectrometry for the stable isotope analysis of plant and soil waters, *Rapid Commun. Mass
34 Spectrom.*, 25(20), 3071–3082, doi:10.1002/rcm.5204, 2011.
- 35 Zimmermann, U., Ehhalt, D. and Muennich, K. O.: *Soil-Water Movement and
36 Evapotranspiration: Changes in the Isotopic Composition of the Water.*, in *Isotopes in
37 Hydrology.*, pp. 567–85, International Atomic Energy Agency, Vienna, Austria., 1968.

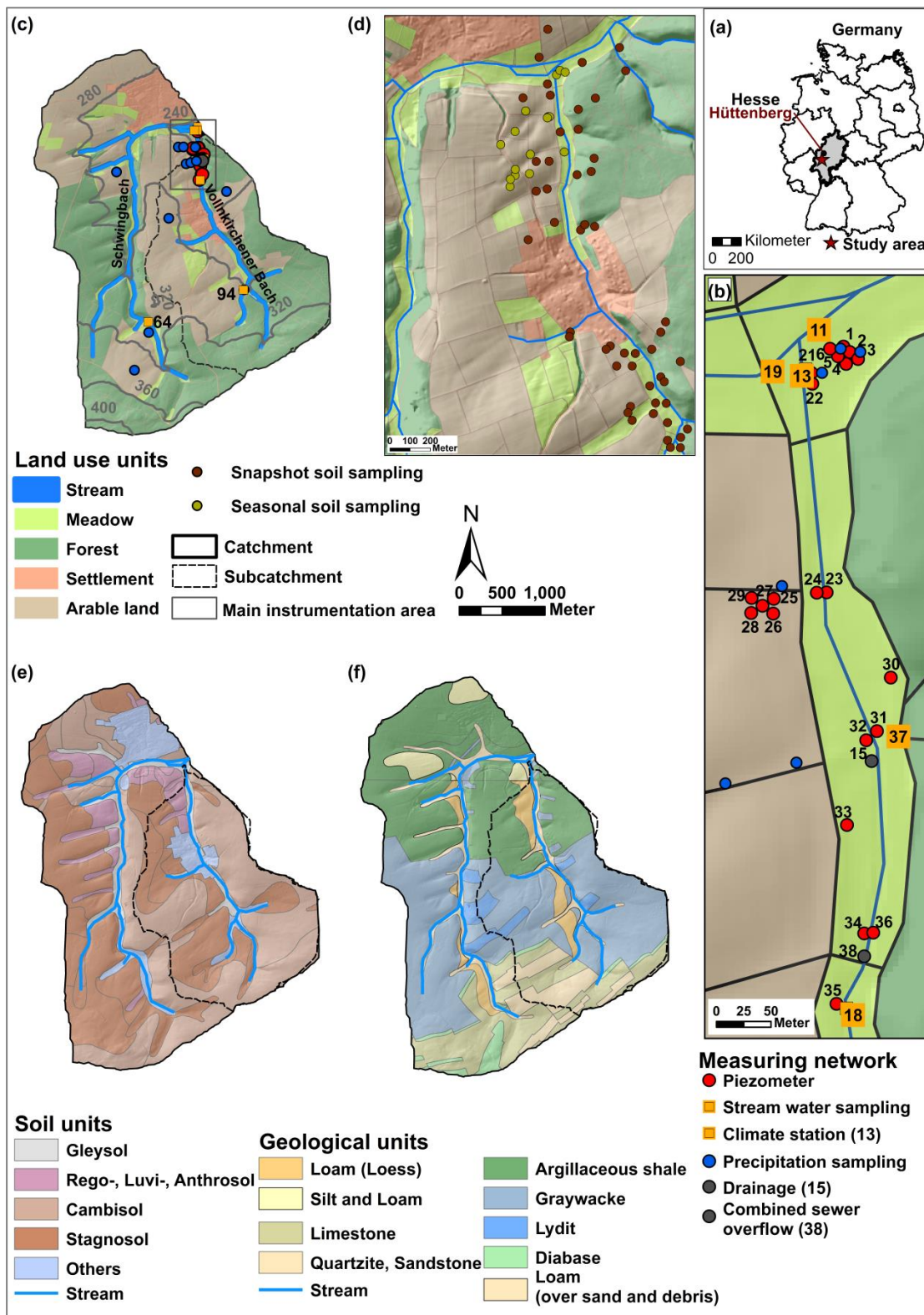
38

1 Table 1. Descriptive statistics of $\delta^2\text{H}$, $\delta^{18}\text{O}$, and d-excess values for precipitation, stream, and
 2 groundwater over the two-year observation period including all sampling points.

Sample type	Mean \pm SD		Min		Max		D-excess mean \pm SD	N
	$\delta^2\text{H}$	$\delta^{18}\text{O}$	$\delta^2\text{H}$	$\delta^{18}\text{O}$	$\delta^2\text{H}$	$\delta^{18}\text{O}$		
	[‰]	[‰]	[‰]	[‰]	[‰]	[‰]		
Precipitation	-43.9 \pm 23.4	-6.2 \pm 3.1	-167.6	-22.4	-8.3	-1.2	5.9 \pm 5.7	592
Vollnkirchener Bach	-58.0 \pm 2.8	-8.4 \pm 0.4	-66.3	-10.0	-26.9	-6.7	9.0 \pm 2.3	332
Schwingbach	-58.2 \pm 4.3	-8.4 \pm 0.6	-139.7	-18.3	-47.2	-5.9	9.0 \pm 2.2	463
Groundwater meadow	-57.6 \pm 1.6	-8.2 \pm 0.4	-64.9	-9.2	-50.8	-5.7	7.9 \pm 5.5	375
Groundwater arable land	-56.2 \pm 3.7	-8.0 \pm 0.5	-91.6	-12.3	-49.5	-6.8	1.7 \pm 5.0	338
Groundwater along stream	-59.9 \pm 6.8	-8.5 \pm 0.9	-94.5	-13.0	-49.5	-7.0	8.2 \pm 1.5	108

1 Table 2. Mean and standard deviation for isotopic signatures and soil physical properties in 0.2 m and 0.5 m soil depth (N = 52 per depth).

	$\delta^2\text{H}$ [‰]		$\delta^{18}\text{O}$ [‰]		water content [% w/w]		pH		bulk density [g cm ⁻³]	
	0.2 m	0.5 m	0.2 m	0.5 m	0.2 m	0.5 m	0.2 m	0.5 m	0.2 m	0.5 m
Mean±SD	-46.9±8.4	-58.5±8.3	-6.6±1.2	-8.2±1.2	16.8±7.2	16.1±8.3	5.0±1.0	5.3±1.0	1.3±0.2	1.3±0.2

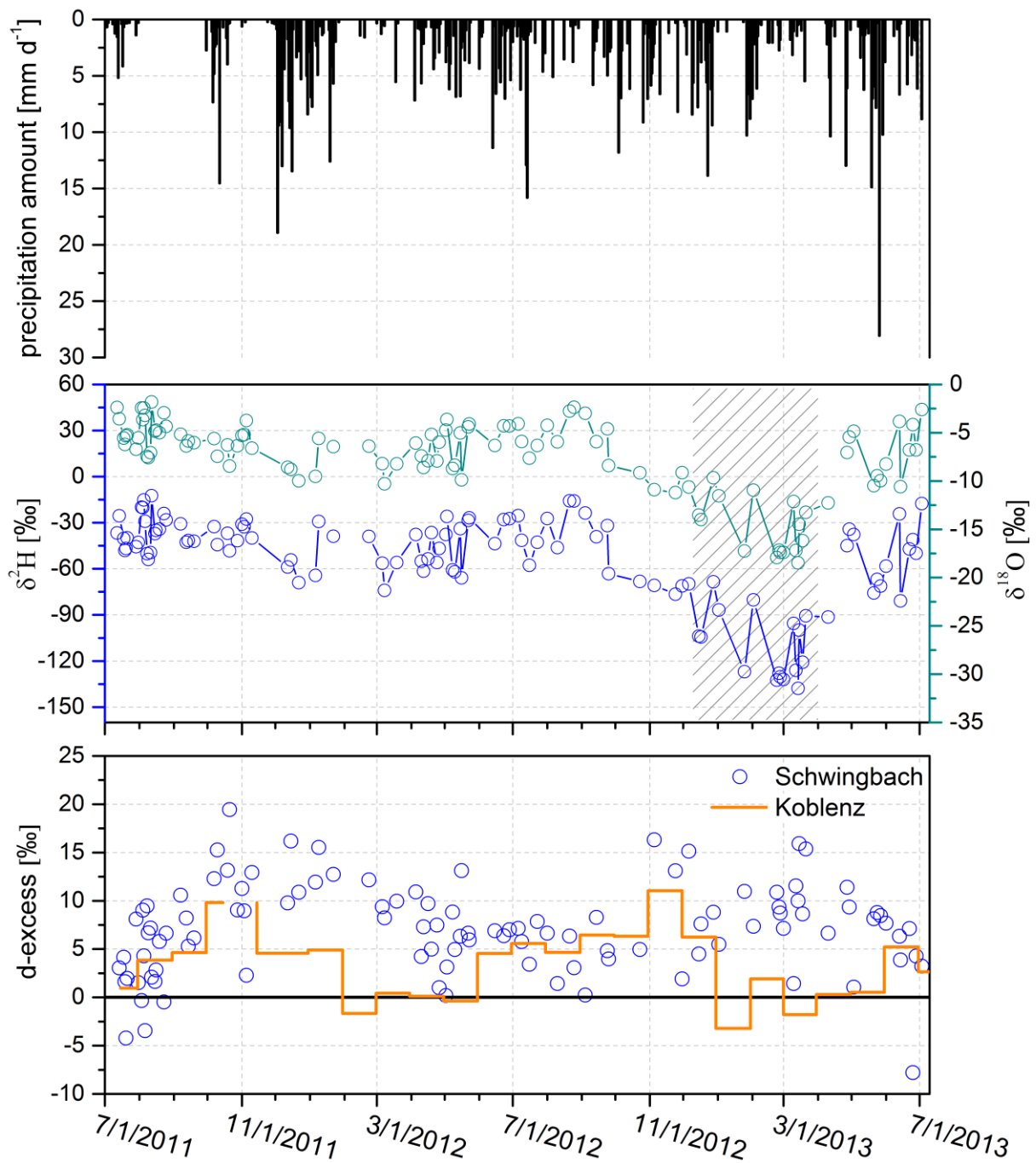


1

2

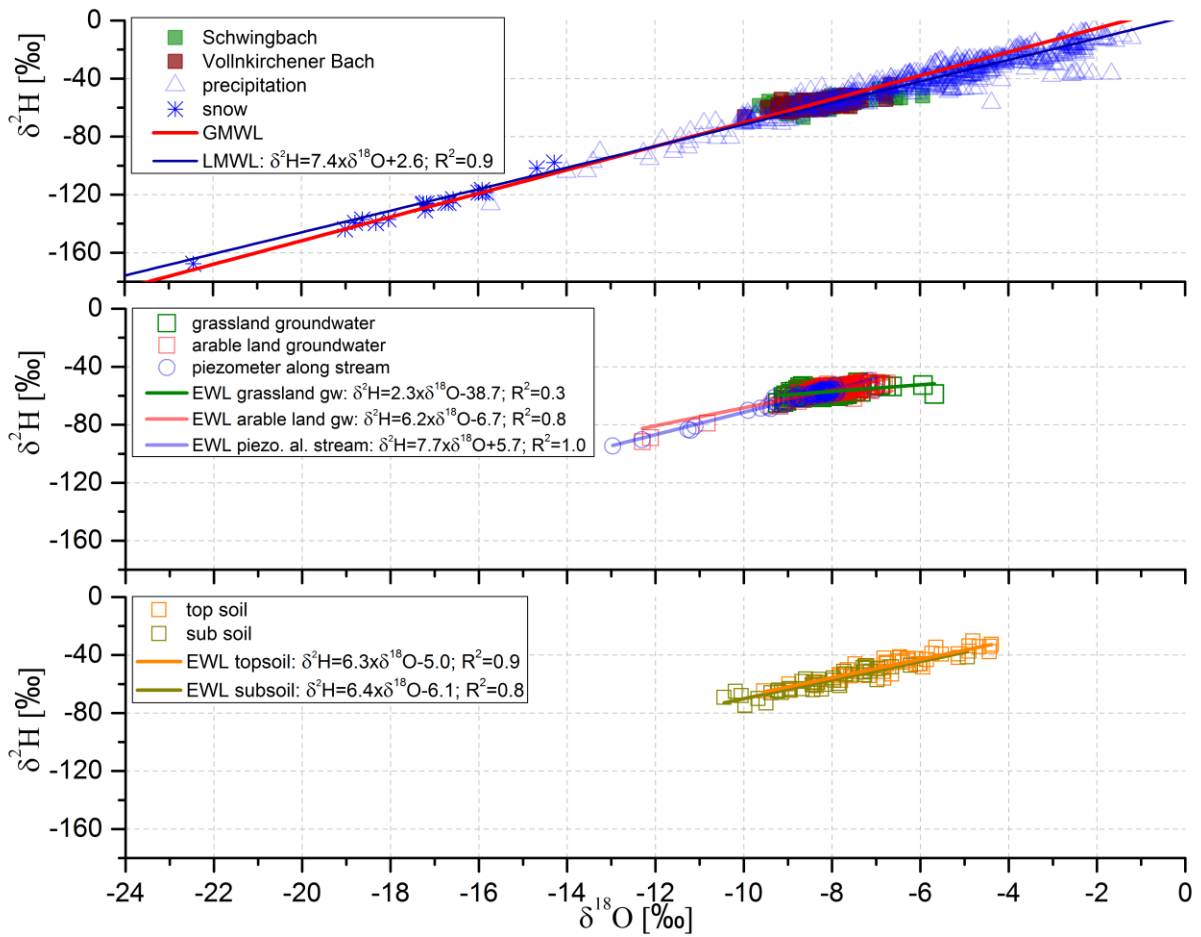
3 Figure 1. Maps show (a) the location of the Schwingbach catchment in Germany, (b) the main
 4 monitoring area, (c) the land use, elevation, and instrumentation, (d) the locations of the

- 1 snapshot as well as the seasonal soil samplings, (e) soil types, and (f) geology of the
- 2 Schwingbach catchment including the Vollnkirchener Bach subcatchment boundaries.
- 3



1
2
3
4
5
6
7

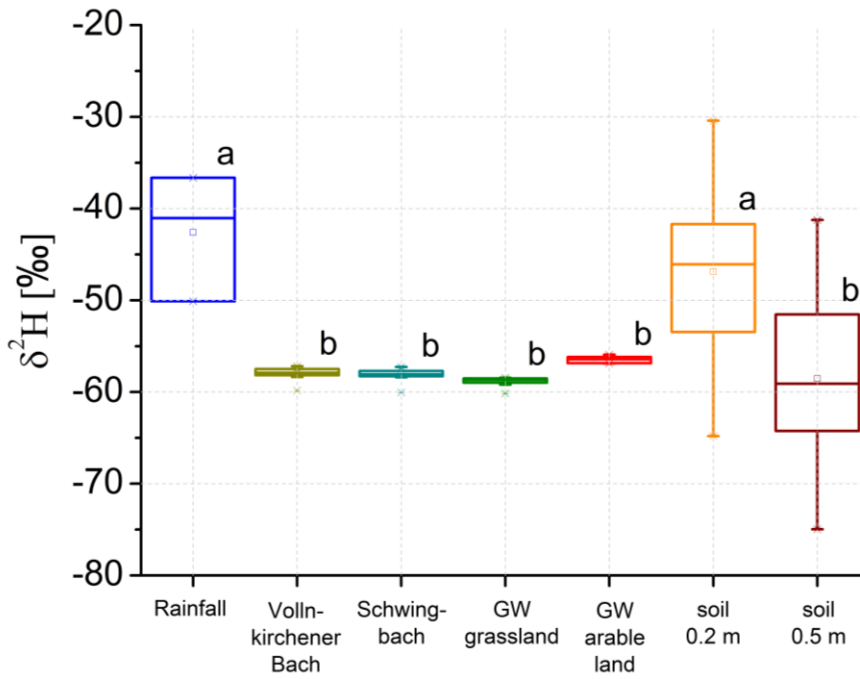
Figure 2. Temporal variation of precipitation amount, isotopic signatures ($\delta^2\text{H}$ and $\delta^{18}\text{O}$) including snow samples (grey striped box), and d-excess values for the study area compared to monthly d-excess values (July 2011 to July 2013) of GNIP station Koblenz with reference d-excess of GMWL ($d = 10$; solid black line).



1

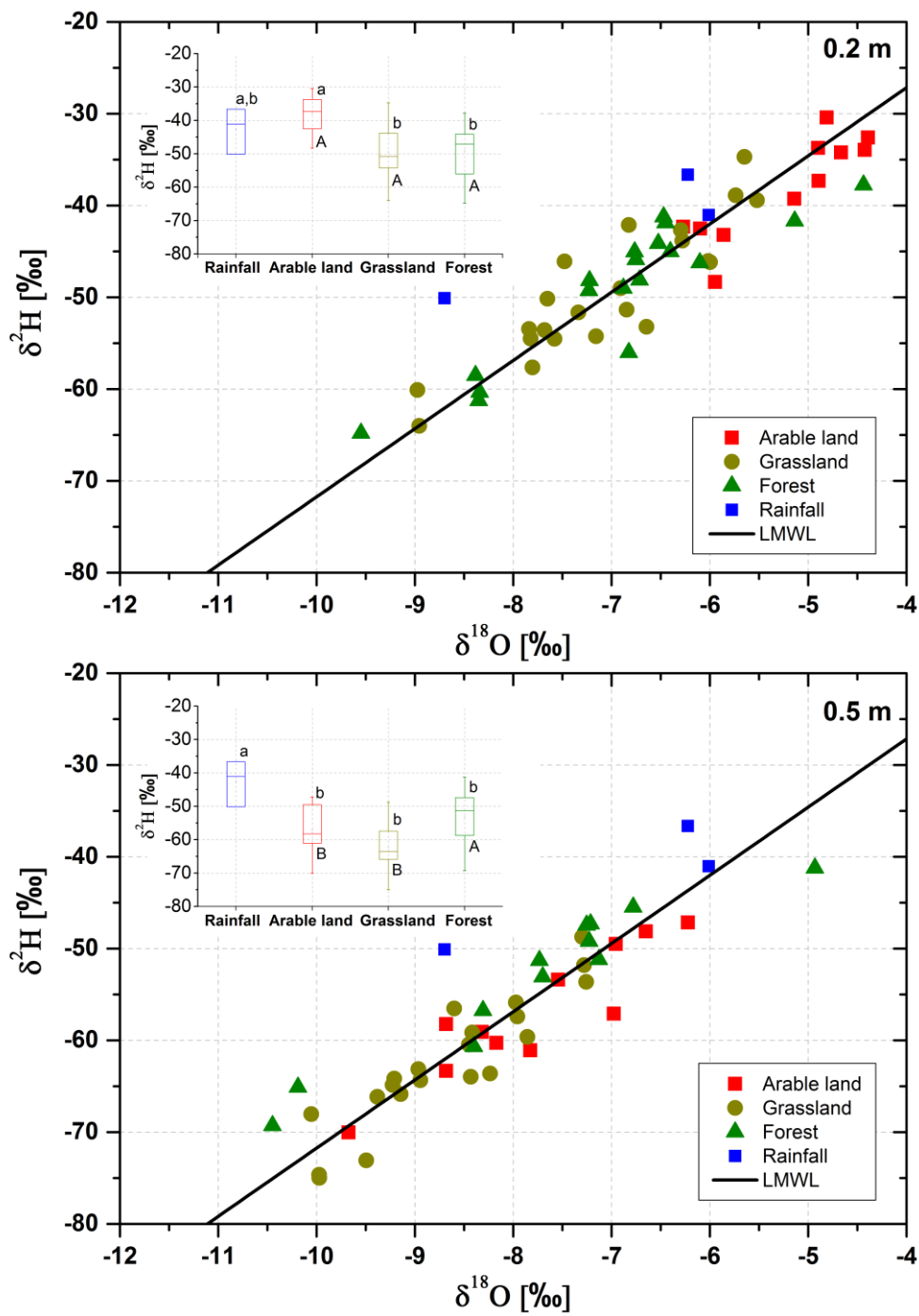
2

3 Figure 3. Local Meteoric Water Line for the Schwingbach catchment (LMWL) in comparison
 4 to GMWL, including comparisons between precipitation, stream water, groundwater, and soil
 5 water isotopic signatures and the respective EWLs.



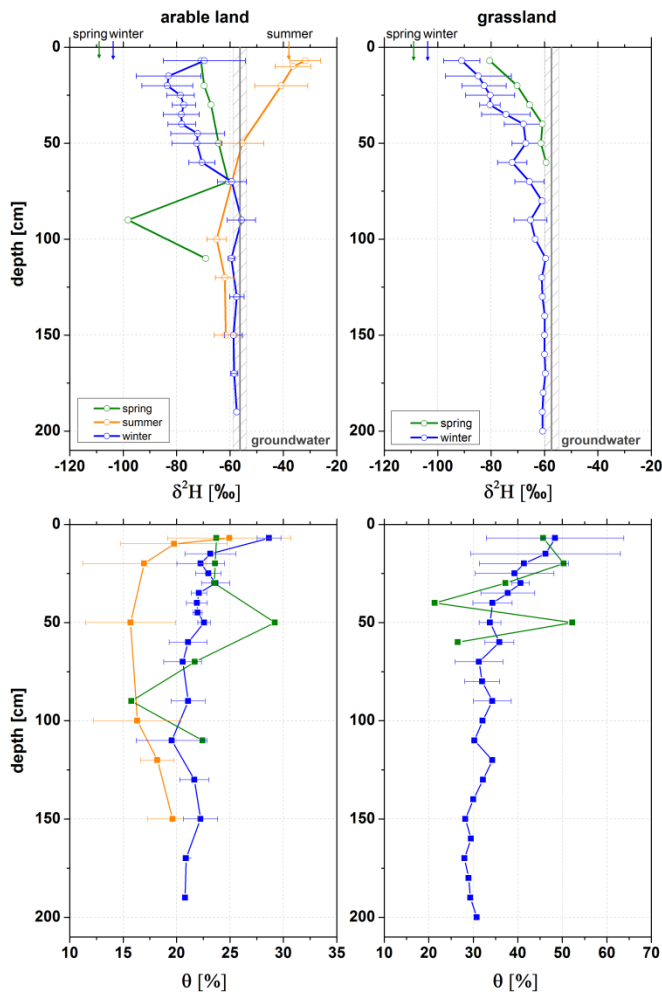
1
2
3
4
5
6

Figure 4. Boxplots of $\delta^2\text{H}$ values comparing precipitation, stream, groundwater, and soil isotopic composition in 0.2 m and 0.5 m depth (N = 52 per depth). Different letters indicate significant differences ($p \leq 0.05$).



1
2

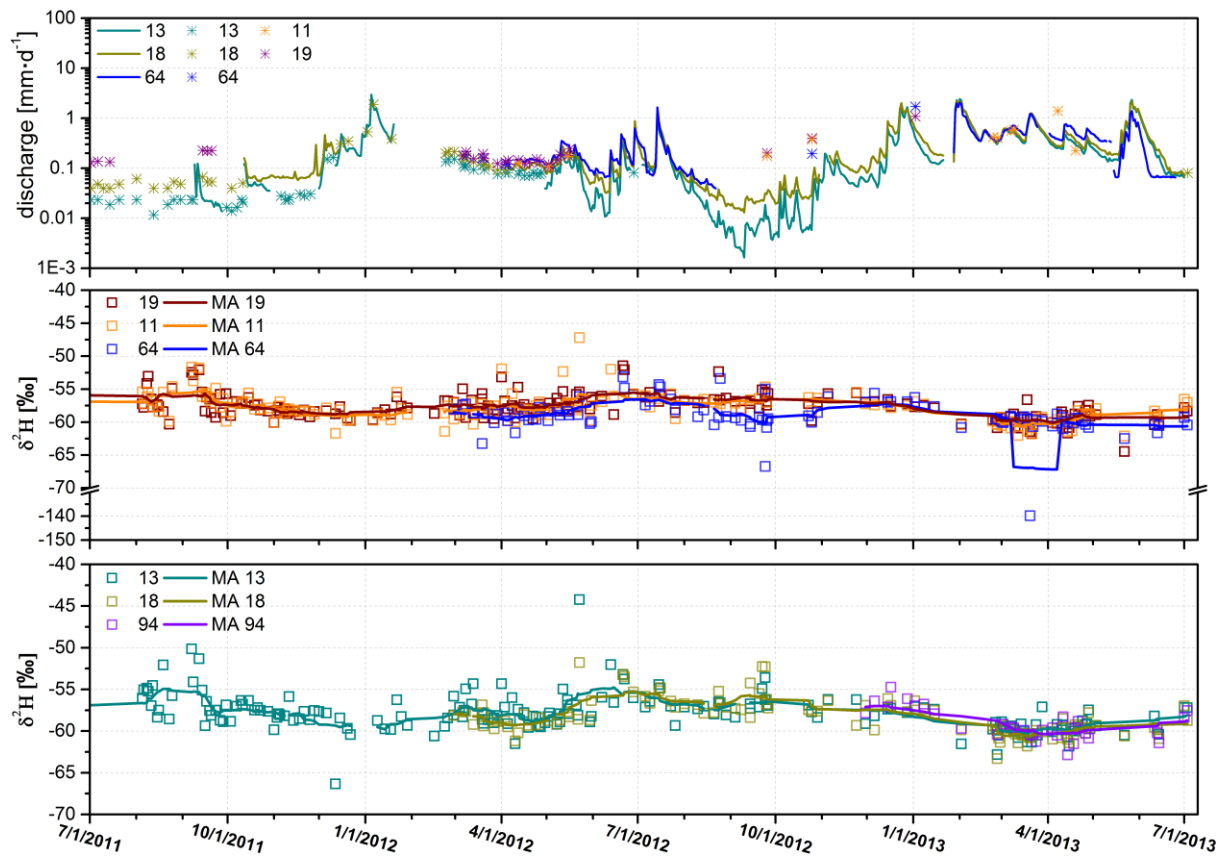
3 Figure 5. Dual isotope plot of soil water isotopic signatures in 0.2 m and 0.5 m depth
 4 compared by land use including precipitation isotope data from 19, 21, and 28 October 2011.
 5 Insets: Boxplots comparing $\delta^2\text{H}$ isotopic signatures between different land use units and
 6 precipitation (small letters) in top and subsoil (capital letters). Different letters indicate
 7 significant differences ($p \leq 0.05$).



1

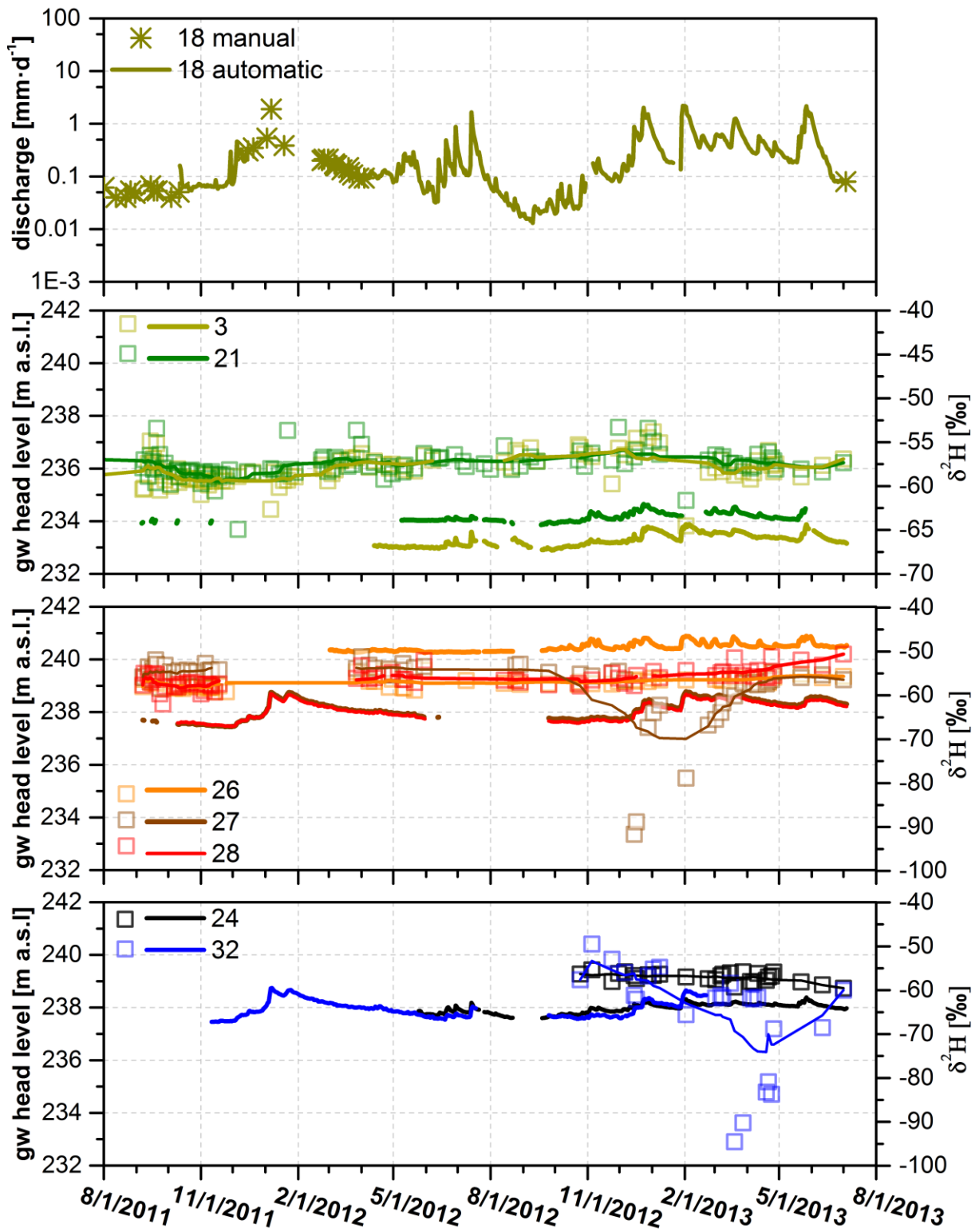
2

3 Figure 6. Seasonal $\delta^2\text{H}$ profiles of soil water (upper panels) and water content (lower panels)
 4 for winter (28 March 2013), summer (28 August 2011), and spring (24 April 2013). Error bars
 5 represent the natural isotopic variation of the replicates taken during each sampling campaign.
 6 For reference, mean groundwater (grey shaded) and mean seasonal precipitation $\delta^2\text{H}$ values
 7 are shown (coloured arrows at the top).



1
2
3
4
5
6
7
8

Figure 7. Mean daily discharge at the Vollnkirchener Bach (13, 18) and Schwingbach (site 11, 19, and 64) with automatically recorded data (solid lines) and manual discharge measurements (asterisks), temporal variation of $\delta^2\text{H}$ of stream water in the Schwingbach (site 11, 19, and 64) and Vollnkirchener Bach (site 13, 18, and 94) including moving averages (MA) for streamflow isotopes.

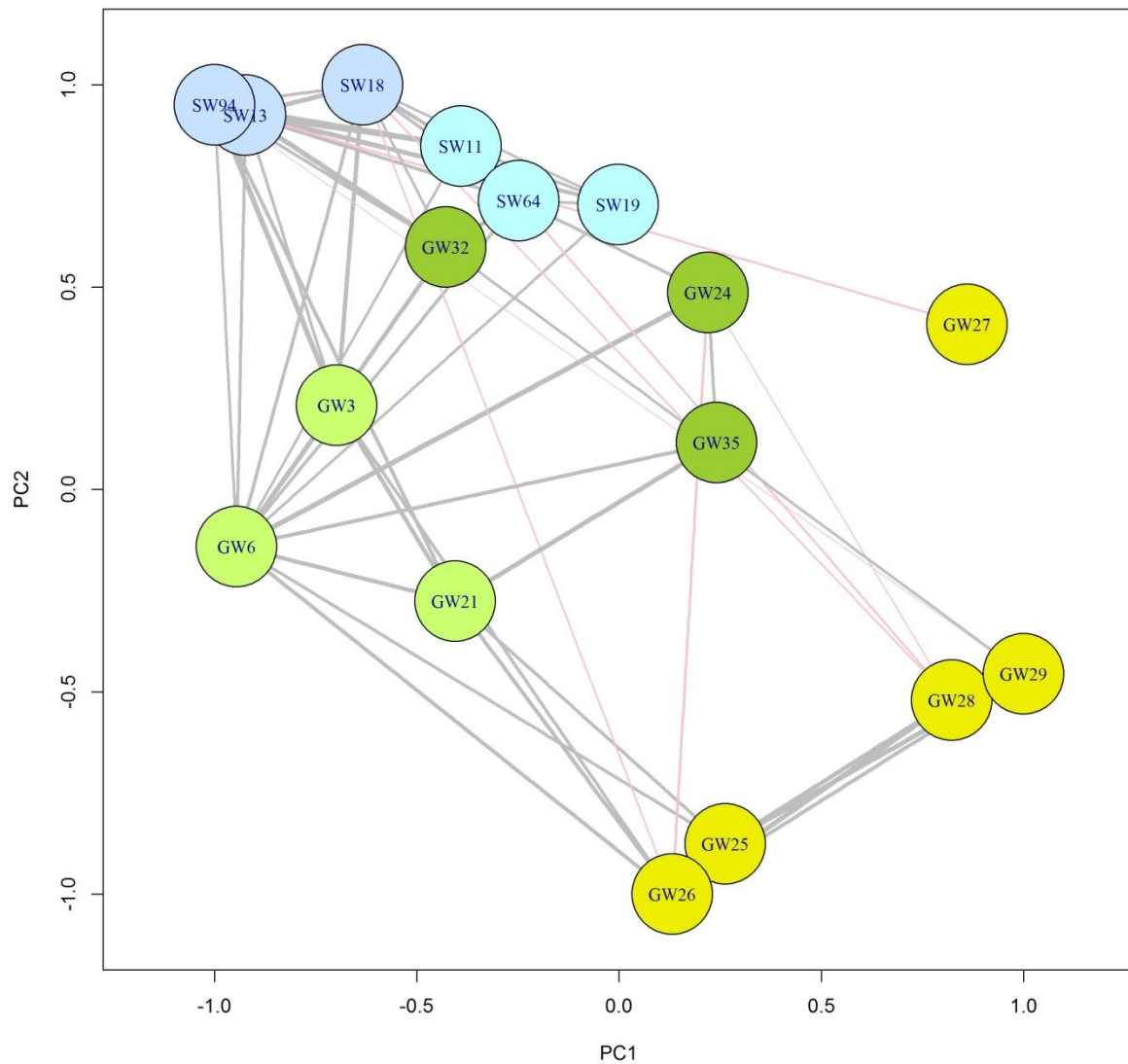


1

2

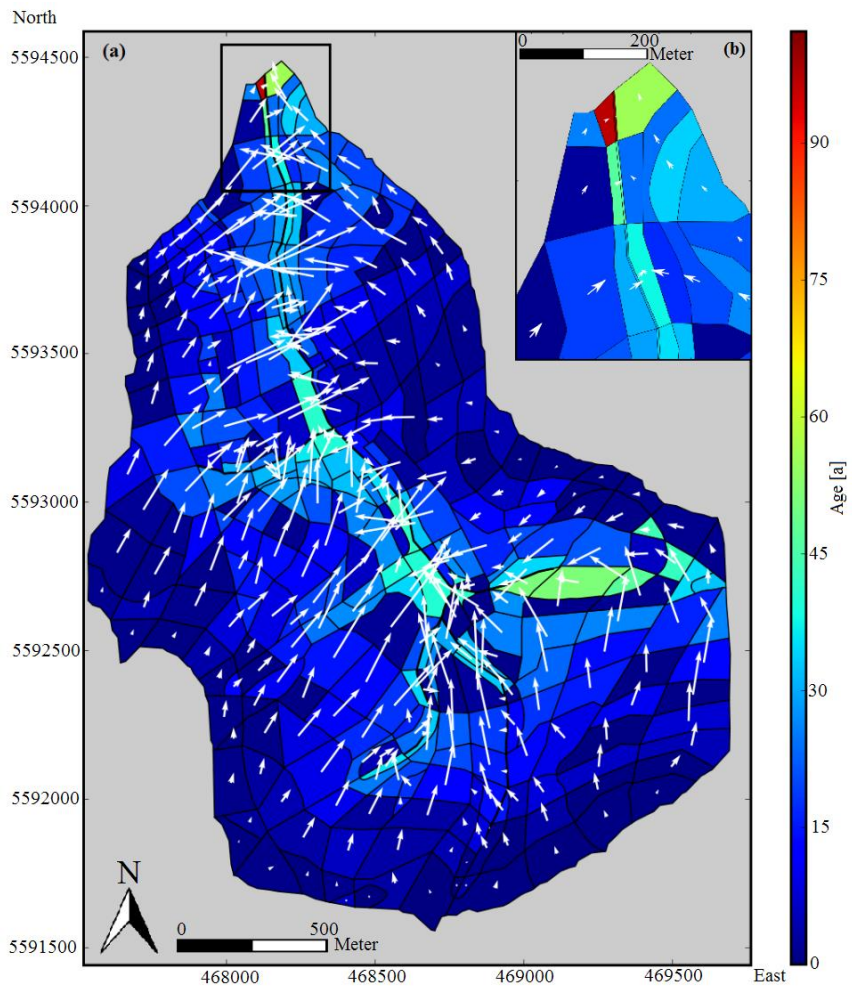
3 Figure 8. Temporal variation of discharge at the Vollnkirchener Bach with automatically
 4 recorded data (solid line) and manual discharge measurements (asterisks) (site 18),
 5 groundwater head levels, and $\delta^2\text{H}$ values (coloured dots) for selected piezometers under

- 1 meadow (site 3 and 21), arable land (site 26, 27, and 28), and beside the Vollnkirchener Bach
- 2 (site 24 and 32) including moving averages for groundwater isotopes.



1
2
3
4
5
6
7
8
9
10
11

Figure 9. Network map of $\delta^{18}\text{O}$ relationships between surface water (SW) and groundwater (GW) sampling points. Yellow circles represent groundwater sampling points on the arable field, light green circles are piezometers located on the grassland close to the conjunction of the Schwingbach with the Vollnkirchener Bach, and dark green circles represent piezometers along the Vollnkirchener Bach. Light blue circles stand for Schwingbach and darker blue circles for Vollnkirchener Bach surface water sampling points. See Figure 1 for an overview of all sampling points. Only statistically significant connections between $\delta^{18}\text{O}$ time series ($p < 0.05$) are shown in the network diagram.



1
2
3
4
5
6

Figure 10. Maps of modelled groundwater ages (colour scheme) and flow directions (white arrows) of (a) the Vollnkirchner Bach subcatchment and (b) detail view of the northern part of the subcatchment. The intensity of flow is depicted by the length of the white arrows.